Pharm Res (2021) 38:851–871
https://doi.org/10.1007/s11095-021-03043-7

RESEARCH PAPER

Novel Curcumin-Resveratrol Solid Nanoparticles Synergistically Inhibit Proliferation of Melanoma Cells

Gayathri Heenatigala Palliyage[1] • Noor Hussein[2] • Michael Mimlitz[1] • Catherine Weeder[1] • Marya Hassan A Alnasser[2] • Somnath Singh[1] • Andrew Ekpenyong[1] • Amit K. Tiwari[2] • Harsh Chauhan[1,3]

Received: 20 September 2020 / Accepted: 8 April 2021 / Published online: 12 May 2021

ABSTRACT Polyphenols such as curcumin (Cur) and resveratrol (Res) have been recently shown to have potential to inhibit proliferation of highly aggressive melanoma cells. This study was designed to investigate the feasibility of a topical delivery system, using a solid lipid nanoparticles (SLNs) loaded delivery systems, that can enhance the skin penetration and anti-cancer efficacy of combination of these polyphenols. Negatively charged Cur-Res SLNs with a mean diameter of 180.2 ± 7.7 nm were prepared using high shear homogenization method. Cur-Res SLNs were found to be stable up to 2 weeks under 4°C. The in vitro release study showed that Res was released five time more than curcumin. The permeability of resveratrol was about 1.67 times that of curcumin from the SLN-gel formulation which was significantly ($p < 0.05$) lower than from SLN suspension. More than 70% of Cur-Res SLNs were bound to skin locally in a skin binding study suggesting potentially utility of Cur-Res SLNs in the treatment of localized melanoma. In fact, the electrical cell-substrate impedance sensing (ECIS) measurements suggested that Cur-Res combination has potential to stop cell migration of B16F10 melanoma cells. Furthermore, both, Cur-Res SLNs and Cur-Res solution at the ratio of 3:1 demonstrated a strong synergistic inhibition of SK-MEL-28 melanoma cell proliferation. Further evaluation of Cur-Res SLNs in vivo melanoma models are warranted to establish the clinical utility of Cur-Res formulations in melanoma therapy.

Guest Editor: Sheng Qi

✉ Harsh Chauhan
HarshChauhan@creighton.edu

[1] Creighton University, Omaha, Nebraska 68178, USA

[2] Department of Pharmacology & Experimental Therapeutics, College of Pharmacy & Pharmaceutical Sciences, Frederic and Mary Wolfe Center, 3000 Arlington Ave., MS 1015, Toledo, Ohio 43614, USA

[3] School of Pharmacy and Health Professionals, Creighton University, Omaha, Nebraska 68178, USA

KEY WORDS curcumin · electrical cell-substrate impedance sensing · melanoma · nanoparticles · polyphenols · resveratrol

INTRODUCTION

Skin cancer, including both malignant melanoma and non-melanoma, is the most common form of malignancy among the Caucasian population (52). Melanoma skin cancer is the most aggressive type of skin cancer and responsible for the majority of skin-cancer related deaths. As a result of the advances in the understanding of the biology and pathophysiology of melanoma, several new therapies including immunotherapy, cytotoxic chemotherapy, and molecular targeted therapy were introduced in the treatment of melanoma (8). However, the therapies cause severe side effects and toxicities resulting in minimal impact on patient survivability (4). This is where polyphenols, such as curcumin, resveratrol, quercetin, coumarin gained great interest in the anticancer treatments mainly due to their wide spectrum of beneficial properties including anti-inflammatory, antioxidant, anticancer and antiviral effects. Most importantly natural polyphenols are non-toxic molecules. Among all the natural polyphenols, curcumin and resveratrol are the most well-studied compounds in the treatment of melanoma (31). Individually both compounds have shown significant benefits in melanoma, but to the best of our knowledge, no study has been conducted to exploit the synergistic advantage of the combination of curcumin and resveratrol in the melanoma treatment. Furthermore, it has been found that the maximal therapeutic benefits against tumor development could be achieved with combinational therapy by affecting several targets at the same time.

Curcumin (diferuloylmethane), is a yellowish polyphenol derived from the turmeric plant *Curcuma longa* (62). In terms of mechanism of action, it acts on multiple molecular targets involved in melanoma pathogenesis such as Mek/Erk and PI3K/Akt (44), Erk/Akt (12), protein p53, Bcl-2 (29) and

NF-kB (72). Resveratrol (3,5,4′-trihydroxy-trans-stilbene) is naturally extracted from grapes, blueberries, cranberries, and peanuts. It induces the apoptosis and suppresses the melanoma cell proliferation by inhibiting the multiple key signaling pathways including Akt, mTOR (38, 83), Mek/Erk (45), STAT3 and NF-kB (7). However, poor systemic bioavailability and high metabolic instability of curcumin and resveratrol have limited their clinical efficacy in melanoma.

Recently, various penetration enhancement techniques have been developed to enhance the thermodynamic activity and the penetration of poorly soluble compounds. Nanoparticulate drug delivery is one of the most common approaches utilized in topical delivery to enhance the cutaneous penetration of the compounds (18). Numerous biocompatible self-assembled nanocarriers including liposomes (13), lipid carriers (34), hydrogel (76), and nanosponges (5) have been developed to improve bioavailability, antineoplastic efficacy, pharmacological efficacy, and photostability of polyphenols in topical applications and among them lipid nanoparticles (SLNs) have gained great interest in the delivery of hydrophobic and lipophilic polyphenols compared to conventional formulations.

This article aims to design the topical curcumin and resveratrol loaded SLNs (Cur-Res SLNs) using Compritol 888 ATO as a lipid phase. This study hypothesized that topical Cur-Res SLNs will result in higher concentrations of both drugs in the skin which can be translated into beneficial treatments of melanoma. Cur-Res SLNs were further characterized and evaluated for skin binding and in vitro release study. Topical gel base was prepared by incorporating nanoparticle suspension with Carbopol 974P to carry out the Ex-vivo skin penetration studies using shed snake skin. The effects of curcumin solution, resveratrol solution, Cur-Res solution and Cur-Res SLNs on SK-MEL-28 cell confluence were analyzed by IncuCyte cell proliferation assays and MTT assays were carried to calculate the IC50 doses for each treatment. Chou-Talalay method was used to evaluate the synergism of Cur-Res solution and Cur-Res SLNs by comparing drug doses with a fraction of tumor cells affected. The data were analyzed using CompuSyn software to determine the combination index (CI) and dose-reduction index (DRI). Lastly, Electrical cell-substrate impedance sensing (ECIS), an automated method to evaluate the morphological changes of adherent cells in a nanoscale range, was carried out to investigate the inhibitory effects of Cur-Res SLNs and Cur-Res solution on cell migration of B16F10 melanoma cells.

MATERIALS AND METHOD

Material

Curcumin (purity >95%) was purchased from Acros Organics (Geel, Belgium). Resveratrol (99%) was provided by Carbosynth Limited. Compritol 888 ATO was supplied by Gattefossé SAS (San Diego, USA). Poloxamer 188 and Tween 80 were respectively purchased from Corning (New York, USA) and Fisher Scientific (Waltham, USA). Acetone (HPLC grade), Methanol Optima ®, and Ethanol were obtained from Fisher Scientific. Carbopol® 974P NF was purchased from Lubrizol (Wickliffe, USA). PBS tablets were supplied by Sigma-Aldrich (Steinheim, Germany). DMEM, Trypsin-EDTA and all the other reagents required for cell culture were purchased from Mediatech, Inc. (Manassas, USA). All the experiments used deionized water. All other reagents used for this study were commercially available products and of analytical grade.

Method

Preparation of Solid Lipid Nanoparticles

Cur-Res SLNs were formulated by the high shear homogenization method. Compritol 888 was used as solid lipid with poloxamer 188 and Tween 80 being used as surfactant and co-surfactant. In brief, 4.5% *w/v* of Compritol heated to 70°C; above the melting point of the lipid and 0.75% w/v of curcumin and 0.25% w/v of resveratrol dissolved in 2 ml of acetone was added into lipid phase dropwise under continuous stirring. On the other hand, the aqueous phase was prepared by heating 3% *w/v* poloxamer 188, 1.5% w/v tween 80 and 10 ml of distilled water together to the same temperature. The aqueous phase was poured at a steady rate into the lipid phase, at a 20,000 rpm with UltraTurrax. The resultant dispersion was homogenised for 30 min and subjected to probe sonication for 5 min to facilitate the particle formation. The lipid: surfactant: drug ratio is 4.5: 4.5: 1. Cur-Res SLNs were further optimized in preliminary experiments for lipid, surfactant and drug concentrations as well as homogenization and probe sonication time.

To prepare the Cur-Res SLN gel, a specific amount of Carbopol 974P (0.5% *w/v*) was dissolved in distilled water and homogenized at 4000 rpm at room temperature for 20 min to obtain a homogenous phase. Sodium hydroxide (2 M) was added to Carbopol solution drop-by-drop which resulted into a gel matrix with pH 5.4. The calculated amount of freshly prepared Cur-Res SLNs dispersion was added to the gel and mixed for 10 min. The prepared gel was centrifuged at 4000 rpm for 20 min to remove the air bubbles. The Cur-Res gel was placed in the refrigerator for overnight before using for study.

Physiochemical Characterization of SLNs

Samples were prepared for particle size analysis by diluting 100 µl of the SLN dispersion with 2 ml deionized water. Zeta

potential analysis was done by diluting 100 µl of the SLN dispersion with 5 ml deionized water. Zeta potential analyser (Brookhaven Instruments Corporation, USA) was used analyse the particle size and zeta potential of the resultant SLN dispersion. The XRD studies for curcumin SLNs (1% *w/v*), resveratrol SLNs (1% w/v), Cur-Res SLNs (0.75:0.25% w/v), as well as blank SLNs were carried out. The crystallinity of the samples was analyzed using PANalytical Empyrean Diffractometer (Almelo, the Netherlands). The samples were exposed to CuKα radiation at 40 kV and 45 mA and scanned over 2θ range 5–60° with a step size of 0.05°.

UV-Visible Spectral Analysis

Simultaneous quantification of curcumin and resveratrol was carried out by UV-visible spectrophotometer (BioTek Instruments, USA). The standard stock solutions (20 µg/ml) of curcumin and resveratrol were freshly prepared by dissolving the polyphenols in ethanol. The wavelength of maximum absorption (λ_{max}) of curcumin and resveratrol was determined by scanning them in the range of 250–700 nm. The stock solutions of curcumin and resveratrol were serially diluted in the concentration range of 60–0.9375 µg/ml to plot the calibration curves. Simultaneous equations for quantification of curcumin and resveratrol were developed based on the equations derived from the standard calibration curves. The UV method was validated for specificity, linearity, precision, accuracy, limit of detection (LOD) and limit of quantitation (LOQ).

Encapsulation Efficiency and Drug Loading

$$\text{Encapsulation efficiency (\%)} = \frac{(\text{Total drug content} - \text{drug content in supernatant})}{\text{Total Drug content}} \text{ x } 100$$

$$\text{Drug Loading Capacity (\%)} = \frac{(\text{Total drug content} - \text{drug content in supernatatnt})}{\textit{Amount of drug + excipients added to the formulation}} \text{ x } 100$$

The encapsulation efficiency and drug loading for Cur-Res SLNs were performed as described by Bhatt P et al. (9). Briefly, 1 ml of Cur-Res suspension was transferred into 10 ml scintillation vial and diluted to 11 ml with deionized water. This suspension was ultrasonicated for 5 min and centrifuged at 4000 rpm for 30 min at 4°C. The supernatant was filtered through a 0.2 µm syringe filter and analyzed for the drug content using UV Spectroscopy. This test was done in triplicate and following formulas were used to analyze the encapsulation efficiency (%) and drug loading capacity, respectively.

Stability Studies

Physical stability of the SLNs was carried out under two different conditions; ambient condition (room temperature) and refrigerated condition (4°C) for three weeks using Cur-Res SLNs (0.75: 0.25% *w/v*) and Blank SLNs. All the suspensions were stored in closed scintillation vials at the aforementioned two temperatures. At specific intervals of time, samples were vortexed and sonicated for 5 min to obtain the homogeneous samples prior to take the aliquots for particle size analysis.

In-Vitro Release Study

In-vitro release studies were carried out using Slide-A-Lyzer dialysis cassettes (MWCS 10,000 Da, Life Technologies Corporation, USA). Cassettes were immersed in the dialysis buffer for 1–2 min to hydrate the membrane. The cassettes were removed from buffer and tapped the edge of the cassettes gently on paper towels to remove the excess liquid. The amount of 2 ml SLN suspension was withdrawn from a syringe and transferred into the cassette cavity via inserting the syringe needle through the ports located at the top corner of the cassette. The plunger of the syringe was pulled on to draw the excess air from the cassette cavity into the syringe. Flotation buoy/flotation device was attached to the dialyze cassette to enhance the flotation of the cassette in the medium. This was then immersed in a glass vial containing 200 ml release medium (Phosphate buffered saline (PBS), pH 7.4). The stirring rate and temperature were kept at 400 rpm and 37°C. At different time intervals, 500 µl aliquoted of the receptor medium was withdrawn and replaced with an equal volume of fresh medium. Samples were diluted with methanol (50:50% *v*/v) and analyzed by UV vis spectrophotometer at 306 and 420 nm. The cumulative release percentage of curcumin and resveratrol was calculated.

Determination of Binding of Curcumin-Resveratrol with Shed Snake Skin

The shed snake skin (*Pituophis melanoleucus lodingi*) were obtained from local Henry Doorly Zoo, Omaha, NE and stored in the freezer −20°C until usage. Snakes shed epidermal layer which thickness can vary (e.g. 10–40 µm) depending on its species (42). The snake skin was taken out from the freezer and pulverized in a mortar with a pestle. The pulverized skin particles (50 mg), passing through a 40-mesh sieve but retained by a 60-mesh sieve, was mixed with 1 ml from the Cur-Res SLNs (0.75:0.25% *w/v*) dispersion by vortexing. The similar amount of Cur-Res solution (0.75:0.25% w/v) was used as a control. Both dispersions were prepared using deionized water. The mixture was shaken for 24h at 37°C. After 24h. of contact time, it was

poured into two falcon tubes and centrifuged for 20 min at 1500 rpm. This step was repeated for two more times after washing with the dispersion medium to remove the unbound drug. The supernatant was collected for the quantification of the drug by using UV spectrophotometer. The amount of the drug that bound to the skin was obtained by subtracting the amount of the drug recovered in supernatants from the amount of the drug initially added.

Determination of Permeability of Curcumin-Resveratrol through Shed Snake Skin

The skin penetration study of curcumin and resveratrol through shed snake skin was performed using Franz diffusion cells with a penetration area of 0.785 cm^2. Before 24 h of the experiment, skin samples were cut from the dorsal side of shed skin and hydrated at 37°C for overnight in receptor medium (7.4 PBS: ethanol; 70:30% *v*/v). The hydrated snake skin was mounted in between donor and receptor compartment of Franz diffusion cell with stratum corneum of snake skin facing towards the donor compartment. The amount of 600 µL of Cur-Res gel were placed in the donor compartment. The receptor compartment was filled with 5 ml of the mixture of pH 7.4, PBS and ethanol (70:30% *v*/v), stirred with magnetic bar at a 40 rpm and 37°C. At specific time points (1, 4, 6, 8,12, 24, and 48 h), 0.5 ml of receptor medium was withdrawn and analyzed for curcumin and resveratrol concentration by UV method. After sampling, an equal volume of fresh medium was added to the receptor compartment to maintain a constant volume. The qualitative analysis of samples after 48 h was carried by ESI MS in Q1 negative mode. The samples were detected in three replicates, and the results were expressed as the mean ± SD of triplicate experiments.

Electrical Cell Substrate Impedance Sensing

B16F10 cell line (ATCC CRL-6475) was purchased from American Type Culture Collection (Manassas, VA, USA) and maintained in Dulbecco's Modified Eagle's Medium (DMEM) supplemented with 10% fetal bovine serum. The cells were cultured in an incubator with an atmosphere of 5% CO_2 at 37°C in 25cm^2 culture flasks. The effects of Cur-Res SLNs (0.06:0.02 mg/ml) on cell proliferation and migration were tested using five different samples. Table I shows the concentrations of each sample used for ECIS assay. The 8W10E was utilized to carry out cell migration studies of B16F10 cell line. As indicated on Table II, ECIS assay was conducted using eight different conditions. ECIS slide was incubated for about 10 mins with a cell culture medium. Afterward, the medium was removed and each well of the slide was seeded as given in Table II. First, two wells remained sample free and cell-free as reference. The slide was incubated for 4 days and the resistance signal was monitored during the time.

Growth Inhibition Assay

Inhibition of cell growth in response to curcumin, resveratrol and Cur-Res solution, and SLNs was determined using the (3-(4,5-dimethylthiazol-2-yl)-2,5-diphenyltetrazolium bromide) (MTT). Cells were grown in Dulbecco's Modified Eagle Medium (DMEM) with 4.5 g glucose supplemented with 10% fetal bovine serum (FBS) and 1% penicillin/streptomycin (P/S). SK-MEL-28 cancer cell lines were resuspended in DMEM after harvesting the cells with 0.25% trypsin +2.2 mM EDTA. The cells were seeded evenly (180 µL/well) at a density of 5000 cells/well in 96 well plates (Corning, New York) with triplicates. After 24 h of plating, cells were incubated with 180 µL of serial dilutions of the curcumin solution, resveratrol solution, Cur-Res solution, and Cur-Res SLNs at the concentrations given in Table III using DMSO (0.1% *v*/v). Blank SLNs were used as control. The plates were then incubated for another 96 h. Cell proliferation rate was monitored by analyzing the degree of confluency over the time. Afterwards, algorithm in the IncuCyte® software creates the growth curves based on the data points acquired during 24 h intervals over the 4 days. At the end of the 96 h incubation period, 20 µl of MTT (4 mg/ml) was added to each well to terminate the reaction. The plates were incubated for an additional 4 h at 37°C. The culture medium was then discarded. The formed formazan crystals were dissolved by adding 100 µL of DMSO to each well. The absorbance was determined using a SpectraMAX iD3® Multi-mode microplate reader (Sunnyvale, CA, USA) at 570 nm. The IC_{50} was determined using the Bliss method, which is based on the change in the percentage of viable cells after the addition of chemotherapeutic drugs, with or without the reversal compounds.

Evaluating Synergism

Chou-Talalay method was used to evaluate the synergism of Cur-Res solution and Cur-Res SLNs by comparing drug doses with fraction of tumour cells affected. The data were analysed using CompuSyn software in order to determine combination index (CI), median effective dose (dm), and dose-reduction index (DRI).

Table I Composition of the nanoparticles and controls

Formulation/Solution	Cur Conc (mg/ml)	Res Conc (mg/ml)	DMSO Conc (v/v%)	Poloxamer Conc. (mg/ml)	Tween Conc.(mg/ml)	Compritol Conc. (mg/ml)
Blank SLNs	–	–	–	30	7.5	45
Cur-Res SLNs	0.06	0.02	–	30	7.5	45
Cur-Res Sol	0.06	0.02	0.1	–		
Cur Sol	0.06		0.1	–		
Res Sol		0.02	0.1	–		

Statistical Analysis

Statistical analysis was performed using OriginPro. One-way ANOVA was used for significant testing, and the results with a P value less than 0.05 was considered to be statistically significant. Data represent the mean of three independent experiments. The significance level between groups are indicated by the asterisks as follows; $*P < 0.05$, $**P < 0.01$, $***P < 0.001$.

RESULTS AND DISCUSSION

Physiochemical Characterization of SLNs

The LOD and LOQ were found to be 1.09 and 3.33 µg/ml for curcumin and 0.71 and 2.16 µg/ ml for resveratrol. Curcumin showed its maximum absorbance at a wavelength of 424 nm, and that for resveratrol was 306 nm (Supplemental Fig. 2). Further characterization of SLNs was carried out by particle size and analysis and zeta potential. Both blank and Cur-Res SLNs were characterized by a mean diameter of 160.16 ± 1.12 nm and 180.17 ± 7.69 nm, respectively. It is found that particles with small mean diameters (<200 nm) enhance the penetration of drug across the skin (66). The total drug amount to lipid ratio in the present study found to be 1:4.5. The similar method and composition (Compritol 888, tween 80, and poloxamer 188) were used by Gokce et al. (28) to prepare the resveratrol loaded SLNs. The resveratrol loaded SLNs were approximately 161 ± 2.7 nm with the 1:30 drug to lipid ratio. Shelat et al. (68) obtained similar results using Compritol based curcumin loaded SLNs in improving bioavailability of drugs and results indicated that particle size lies between 200 and 300 nm with the 1:20 drug to lipid ratio. Figure 1 (a) demonstrates the macroscopic aspect between blank and Cur-Res SLNs suspensions. Macroscopically, blank and Cur-Res loaded solid lipid nanoparticles showed a homogeneous suspension aspect with a milky white and mustard colour respectively.

Zeta potential (ZP) can be used to measure the surface charge of the particles. It indicates the degree of electrostatic repulsion or attraction between charged particles in the SLN dispersion. These repulsion forces are responsible for preventing aggregation of the nanoparticle. Therefore, ZP (±) can serve as a useful indicator to predict the long-term stability of the SLN dispersion (22). In general, particles with high zeta potential value (Ex. less than −30 mV and more than +30 mV) are less likely to aggregate resulting good physical stability. The physical stability of the nanoparticle decreases with a reduction in zeta potential (23).

Zeta potential value for Cur-Res SLNs was above −30 mV indicating good physical stability and dispersion quality. Both surfactants used in this study were non-ionic. Therefore, slightly ionized fatty acids from glyceryl behenate (Compritol 888) should be responsible for the negative zeta potential value. These findings agree with the results obtained in the Hu et al. (35) study. The zeta potential data for Cryptotanshinone loaded SLNs (CTS-SLNs) range around −27 mV. The author reported that the negative charge of the nanoparticle was

Table II Composition of each well in ECIS array

Code No	Condition	Formulation (µl)	Control (µl)	B16 (µl)	DMEM (µl)
1	B16F10 + DMEM	–	–	500	500
2	Cur-Res SLNs + DMEM	500			500
3	Blank SLNs + B16F10-DMEM	500		500	
4	Cur-Res SLNs + B16F10-DMEM	500		500	
5	Cur-Res Sol + B16F10-DMEM		500	500	
6	Cur Sol + B16F10-DMEM		500	500	
7	Res Sol+ B16F10-DMEM		500	500	
8	Cur-Res SLNs + B16F10-DMEM	500		500	

Table III Concentrations of curcumin and resveratrol and their combinations used in growth inhibition assays

	Single Agent		Combination (Cur-Res Sol. / Cur-Res SLNs)
	Curcumin	**Resveratrol**	
Concentrations (μg/ml)	0.1	0.03	0.1: 0.03
	1	0.33	1: 0.33
	6	2	6: 2
	10	3.3	10: 3.3
	20	6.6	20: 6.6
	30	10	30: 10
	60	20	60: 20

likely caused by the lipid composition of the SLNs, even though tween 80 was used as an emulsifier. These results are in agreement with the studies on paclitaxel loaded SLNs obtained by Deshpande (19).

However, many studies reported that non-ionic surfactants could also be responsible for the negative charge of the surface. Non-ionic surfactants could not ionize in aqueous solution like ionic surfactants. However, according to Naik et al. (51), they are capable of forming a charged layer at particle/water interface due to molecular polarization. Moreover, non-ionic surfactants could also act as steric stabilizers by forming a coat around the surface of nanoparticle (22). In this case, Cur-Res SLNs were stabilized by both electrostatic and steric effects of surfactants. El-Housiny et al. (22) reported that Compritol based Fluconazole-loaded SLNs resulted in negative zeta potential values lie between −21 to −33 mV due to steric stabilization of poloxamer 407. Naik et al. (51) reported that zeta potential became more negative with increase concentration of tween 80 from 0.5–1.0%. These results are in agreement with studies on Efavirenz loaded SLNs obtained by Gupta et al. (30).

It is important to obtain a narrow size distribution to avoid the phenomena of Ostwald ripening. Ostwald ripening is the process where the small particles dissolve in solution and deposit on the larger particles in order to reach a more thermodynamically stable state (74). The process of Ostwald ripening can be minimized via decreasing the polydispersity index of particles (57). The PDI for Cur-Res SLNs was lower than 0.25 which indicates narrow size distribution (16).

Encapsulation Efficiency and Drug Loading Capacity

The samples were analysed by UV-Vis spectrometer at 420 and 306 nm (Table IV). The encapsulation efficiency of curcumin and resveratrol were 92 ± 0.01% and 62.82 ± 0.25% *w*/w respectively.

Encapsulation depends on the lipophilicity of the drug and the drug solubility in the lipid phase. The difference in encapsulation efficiency can be addressed using partition coefficient (Log P) of each compound. Log P valve for curcumin and resveratrol found to be 3.29 and 3.10 respectively. Log P of curcumin is slightly higher than resveratrol, indicating high affinity of curcumin for Compritol compared to resveratrol.

Drug loading (DL) was calculated by the amount of total entrapped drug divided by the total weight of nanoparticles to indicate the encapsulated drug as the percentage of the mass of the nanoparticle. Drug loading for curcumin and resveratrol were 15.35 ± 0.31% and 3.49 ± 0.21% respectively. There was a significant difference between drug loading of curcumin and resveratrol ($P < 0.001$). This can be due to the lower drug to lipid ratio. Friedrich et al. (25) obtained similar DL for curcumin (0.49 ± 0.01 mg/ml) and resveratrol (0.49 ±

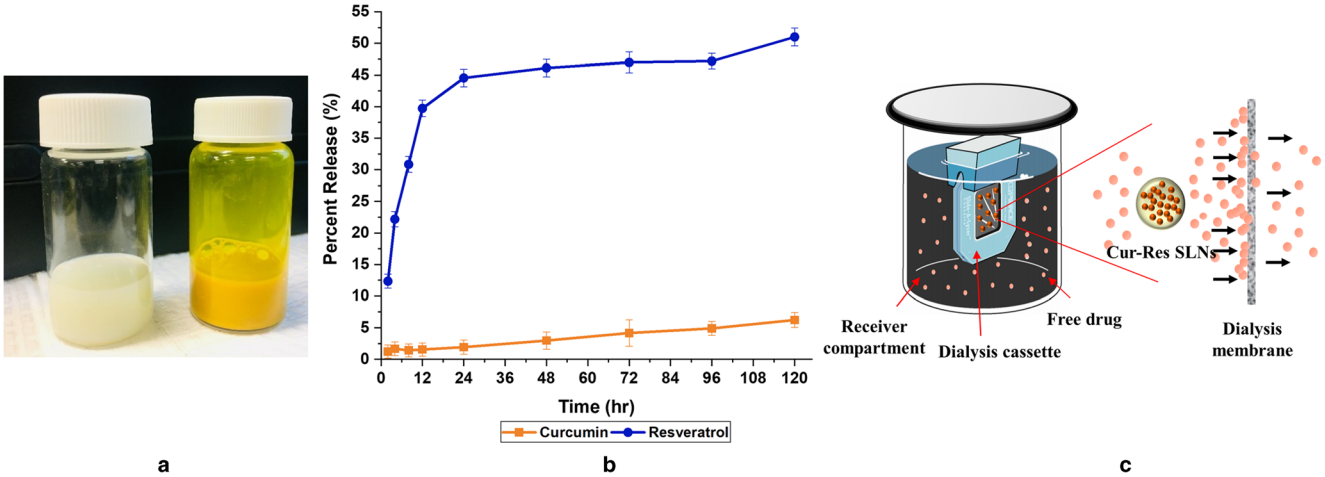

Fig. 1 (a) Schematic illustration of SLN suspension of Blank SLNs (left), Cur-Res SLNs (right); (b) In vitro release profile of curcumin and resveratrol from the Cur-Res SLNs. Data represented as the mean (%) ± SD from three independent experiments; (c) Dialysis method used to analyse the release profile of curcumin and resveratrol.

Table IV Encapsulation efficiency and drug loading for Cur-Res SLNs

	Encapsulation efficiency (%)	Drug loading capacity (%)
Curcumin	92.13 ± 0.01	15.35 ± 0.31
Resveratrol	62.82 ± 0.25	3.49 ± 0.21

0.01 mg/ml) by using lipid-core nanocapsules (LNC) made of sorbitan monostearate and grape seed oil. Their results further demonstrated that the phenomenon of co-encapsulation did not influence the DL and EE% of curcumin and resveratrol individually. Tang et al. (79) investigated the co-delivery of curcumin and piperine by using SLNs made of glycerol monostearate and lecithin. The average DL of curcumin and piperine 19.56 ± 0.18 and 3.26 ± 0.05 µg/mg respectively, with the EE of 87.4 ± 0.6% for curcumin and 14.7 ± 0.2% for piperine.

In Vitro Drug Release

The in vitro release curve for the curcumin and resveratrol in SLNs dispersion in 7.4 pH phosphate buffer at 32°C was shown in Fig. 1 (a). There was a significant ($p < 0.05$) difference between the release kinetics of the two drugs. After 120 h, 51% of resveratrol was released from SLNs whereas less than 10% of curcumin was released from the corresponding SLNs over the same period. The slower release profile of curcumin and resveratrol can be attributed to their distribution in the SLNs. Both curcumin and resveratrol are highly lipophilic compounds, thus they tend to distribute in the lipid core of SLN (15, 53). Pando et al. (55) and Shelat et al. (68) reported the similar "release profile" of SLNs for curcumin and resveratrol.

It is also observed that there is a significant ($p < 0.05$) difference in release profile between curcumin and resveratrol. The difference in release can be attributed to the lipophilicity nature of the curcumin and resveratrol in Compritol 888 constituting the lipid core in the SLNs. The LogP value of Compritol 888 is 9.6 resulting in higher solubility of curcumin in the lipid core (LogP 3.4) compared to resveratrol (LogP 2.9). Also, curcumin is poorly soluble in release medium (phosphate buffer pH 7.4) compared to resveratrol. As a result, that curcumin tends to bind with lipid in SLNs than releasing from SLNs (Fig. 1 (c). For similar reason, in-vitro release studies of pure curcumin through dialysis membrane led to the undetectable concentration of curcumin measured through the validated UV method. Based on the LOQ of curcumin, it can be assumed that the concentration was less than 2.16 µg/ml. Similar issues has been observed by various researchers and to increase the curcumin's solubility in the receiver compartment, they utilized modified-release medium such as 50% (*v*/v) ethanol (64) or used direct dispersion method which facilitated more than 70% of curcumin in the in vitro release studies from the nanoparticles (17, 37).

Friedrich et al. (25) reported the similar release profile of curcumin and resveratrol using Cur-Res SLNs made of sorbitan monostearate and poly(e-caprolactone). The study showed that after 24 h, 73% of resveratrol was released from Cur-Res SLNs, whereas only 9.03% of curcumin was released. The release profile of curcumin and resveratrol from the lipid core nanocapsules (LNC) was analyzed and results showed that resveratrol released faster than curcumin and these profiles exhibited 90% of resveratrol release after 24 h and 35% of curcumin release after 72 h (15).

In vivo drug release from SLNs depends on the several factors, including the interaction between lipid membrane and other cell organelles, and enzymatic degradation. Therefore, in vitro release studies could not accurately predict the release behaviour of drugs from SLNs in vivo (86). The release mechanism of SLNs through the skin has not been fully elucidated yet. A number of release mechanisms have been proposed based on the characteristics of nanoparticles. Among them, the mechanism of "vesicle absorption and/or fusion with stratum corneum" seems to be the dominant drug release mechanism for the Cur-Res SLNs. Cur-Res SLNs release the drug to the skin by absorbing it to the stratum corneum's surface or fusing or mixing with the stratum corneum's lipid matrix. However, more studies are required to understand the underlying mechanism of Cur-Res SLNs. Most nano-lipid systems blend with many other excipients other than the lipid matrix which act as water-soluble "pore formers" (70). In the preparation of Cur-Res SLNs, poloxamer and tween 80 were used as surfactants, in addition to Compritol. The ratio between surfactants and lipid matrix was 3.75:4. When the SLNs contact with aqueous media, the water-soluble excipients start to leach out from nanoparticle. More channels for drug and water diffusion would be created as the leaching rate of surfactants into aqueous phase increase, resulting in sustained release of the drug.

Storage Stability

Physical stability of the SLNs can be investigated using various parameters such as particle size, size distribution, zeta potential, and thermal analysis. Among them, a change in particle size is widely utilized as an indicator to determine particle instability (80). It has been found that particle size of the well-stable nanosystem should be lower than 1 µm, increase in particle size greater than 1 µm causes agglomeration resulting in physical instability (33).

The size of Cur-Res SLNs and blank SLNs was detected for 21 days at two different temperatures; 25°C and 4°C. Particle size of Cur-Res SLNs stored at room temperature was significantly increased from 200 to 500 nm by day 4. This might be due to the aggregation of the vesicles. However, after day 5, it

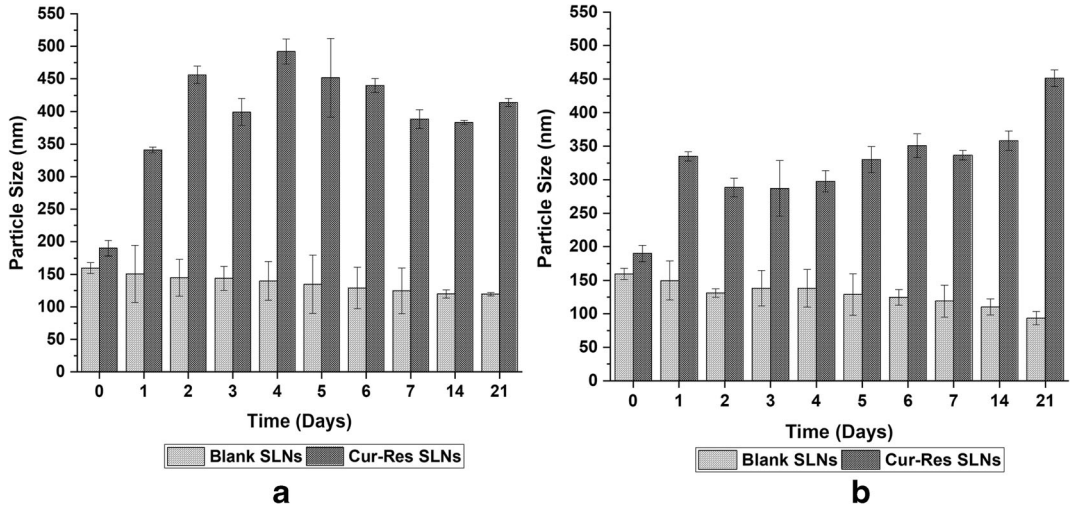

Fig. 2 Storage stability analysis of SLNs at (a) 25 °C and (b) 4 °C.

started to decrease. The particle size was around 400 nm after 21 days. In contrast, particle size of blank SLNs stored at 25°C was gradually reduced over the 21 days (Fig. 2 (a)). Particle size of Cur-Res SLNS wasn't significantly increased at 4°C until two weeks, indicating that they were more stable at 4°C compared to 25°C. However, the size of SLNs had significantly increased after 14 days. The size of blank vesicles stored at 4°C was gradually decreased over the three weeks (Fig. 2 (b)). The results from Fig. 2 (a) and (b) indicate that particle size of Cur-Res SLNs increased slightly when stored at 4°C. Similar observations were reported by Shah (67). Freitas and Müller (23) conducted a study to investigate the effect of light and temperature on physical stability of the SLNs dispersion. The impact of temperature on Compritol SLNs stabilized with poloxamer 188 were determined by storing SLNs at three different temperatures (8°C, 20°C and 50°C). The results indicated that Compritol SLNs stored at both 20°C and 50°C facilitates the rapid particle growth, whereas those stored at 8°C were stable over the three weeks. The mean particle size only increased from 276 ± 2 to 297 ± 5 nm. The impact of temperature on Compritol SLNs stabilized with poloxamer 188 were determined by storing SLNs at three different temperatures (8°C, 20°C and 50°C). The results indicated that Compritol SLNs stored at both 20°C and 50°C facilitates the rapid particle growth, whereas those stored at 8°C were stable over the three weeks. The mean particle size only increased from 276 ± 2 to 297 ± 5 nm**.**

Generally, aqueous SLNs dispersions are stable for longer period of time (up to 3 years), but due to the crystallization-polymorphic transitions associated with SLNs, some systems showed rapid particle growth over the time. Triglycerides exist in three main crystal modifications, namely unstable α, metastable β', and the most stable β (1). Figure 3 illustrates the Compritol® ATO 888 polymorphic transition in SLNs. According to Brubach et al. (10) and Souto et al. (73), A transition from one polymorphic form to another mainly depends on the crystallization rate and temperature during formulation and storage. Compritol SLNs undergo polymorphic transitions during the process of cooling. The bulk of triglycerides crystalize into unstable imperfect α polymorph during rapid cooling, which transforms into stable β-form via metastable β'- form during storage or destabilization of Compritol SLNs (1). However, transitions of SLNs may lead to an increase in the particle size as the result of flocculation, gelation, and Ostwald ripening (56). As mentioned before, crystallization rate is another factor that facilitates particle growth. It was found that crystallization rate is accelerated with room temperature resulting formation of the single polymorph SLNs. However, at a lower temperature, glycerides crystalize separately with slower crystallization rate leading to produce a complex polymorph SLNs, which contains a mixture of polymorphic modifications. A mixture of polymorphs is more stable compared to a single polymorph SLN. This is why particle size of the Cur-Res SLNs stored at 4°C size was not significantly increased compared to room temperature (24).

X-Ray Diffractometry (XRD)

XRD patterns of pure drugs, blank SLNs, and drug loaded SLNs are shown in Fig. 4 (a) and (b). Many intense diffraction peaks were observed for both curcumin and resveratrol in the region of 5° to 30°, indicating their crystalline structure (Fig. 4 (a)). However, XRD patterns of blank and Cur-Res SLNs did not exhibit several crystalline diffraction peaks but three weak diffraction peaks in the range between 17° and 25°, characterizing the amorphous state of the SLNs (Fig. 4 (b)). According to the results, it is clearly seen that incorporation of drug into nanoparticles enhances the drug amorphization

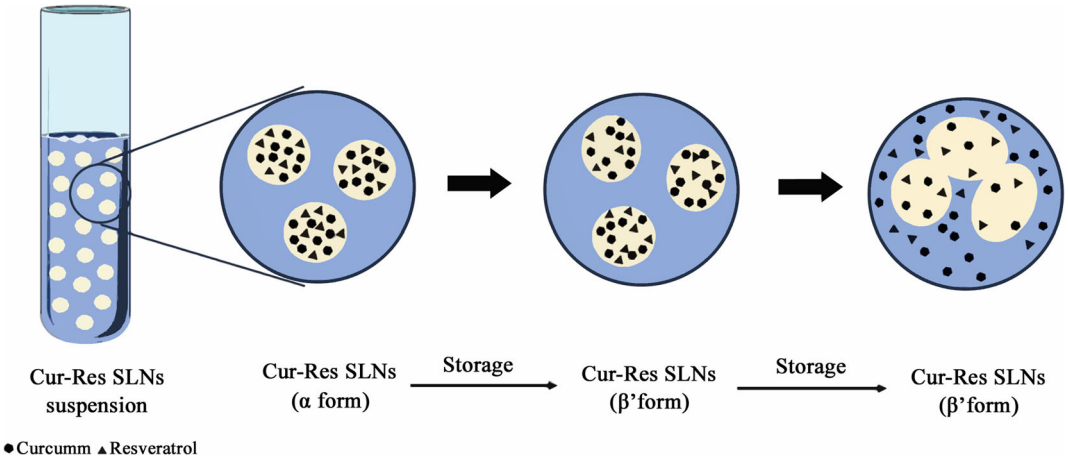

Fig. 3 Polymorphic transitions of Compritol SLNs.

via decreasing the crystalline diffraction peaks of curcumin and resveratrol.

Skin Binding Studies

Figure 4 (c) indicates the percentage of curcumin and resveratrol bound with skin from SLNs or solution containing similar amount of them. Cur-Res SLNs showed 70 ± 0.76% and 75 ± 0.93% binding for curcumin and resveratrol, respectively whereas Cur-Res solution demonstrated significant ($p < 0.05$) increase in binding for resveratrol (97.88 ± 0.56% from solution vs 75 ± 0.93% from SLNs) but no such increase for Cur although both possess Log*P* values greater than 3. Such differences in binding data can be explained on the basis of their Log P values and topological polar surface areas (TPSAs). Resveratrol (log P 3.10) is less hydrophobic than curcumin (log P 3.29) which would result in availability of greater number of free resveratrol molecules from its solution than from SLN formulation where it is entrapped in the lipid particles. This can be the reason for greater skin binding determined for resveratrol from its solution.

In addition, resveratrol from both SLNs and solution showed a higher binding compared to curcumin from both formulations which can be attributed to differences in their TPSAs. The TPSAs for curcumin and resveratrol are 93.1 and 60.7 $Å^2$, respectively which lower values are correlated with permeability/binding with biological membranes. A lower TPSAs for resveratrol might be attributed to its greater binding with skin as corroborated by the similar effect of lower TPSAs of a derivative of methoxyflavone on its greater binding with neuraminidase – a target enzyme inhibition for the treatment of influenza (87).

Moreover, binding of drugs to skin can be attributed to many reasons. As stated in the interim report issued by Environmental Protection Agency, Office of Health and Environmental Assessment and Exposure Assessment Group

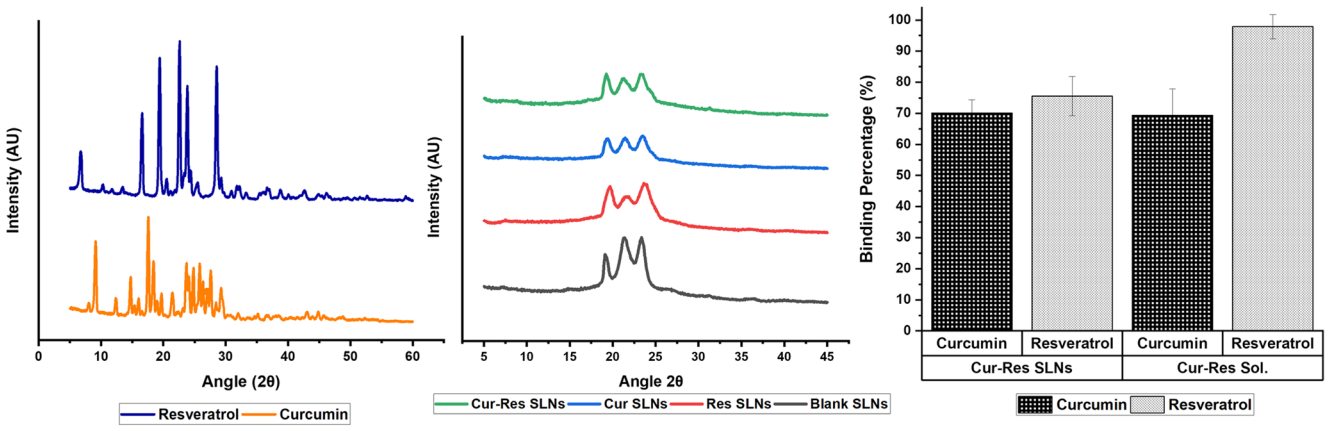

Fig. 4 XRD patterns of (a) pure resveratrol and curcumin (b) drug loaded SLNs; (c) Percentage of drug binding to the skin.

in United States (1992), skin adsorption and penetration of the drug depend on many factors other than their solubility in lipid phase such as chemical structure, compound concentration. Schaefer et al. (65) reported that even small structural difference of compound could cause a significant change in skin adsorption. Furthermore, skin adsorption/binding of the compound could also be influenced by the nature of skin such as skin site, thickness, skin temperature. Further studies are needed to understand the factors that contribute to the difference in binding percentage between curcumin and resveratrol.

Most importantly, this binding experiment was conducted only for 10 h. However, in vitro release data showed that no significant amount of curcumin was released by 10 h due to the lipophilic nature of curcumin towards Compritol. Therefore, in order to better understand the binding behaviors of curcumin and resveratrol from SLNs, any future study should be conducted for more extended period of time through which their release must be exhausted.

Determination of Permeability of Curcumin and Resveratrol through Ex-Vivo Shed Snake Skin

There is considerable interest in developing topical applications of poorly soluble drugs for prevention and treatment of melanoma. Consequently, the goal of the skin permeation study is to determine percutaneous absorption of curcumin and resveratrol and the various formulation parameters influencing it. Such estimation of skin permeability would enable us to manipulate formulation parameters for the desired therapeutic outcomes via systemic bioavailability. A wide range of variability is reported for percutaneous absorption and systemic bioavailability of a drug. Therefore, a factor of difference of three between skin permeability and targeted systemic bioavailability (Curcumin IC_{50}: 6.38 ± 0.27 µg/ml; Resveratrol IC_{50}: 3.67 ± 0.14 µg/ml) would be acceptable for further optimization (36). Shed snake skin was selected as a model membrane (3) is a pure, nonliving stratum corneum containing similar lipid content as human stratum corneum (58).

Table V Steady state flux of curcumin and resveratrol from different formulations through shed snakeskin

	Steady State Flux ($\mu g.cm^{-2}\ h^{-1}$) Mean ± SD	
	Gel	Suspension
Curcumin	0.31 ± 0.08	0.41 ± 0.01
Resveratrol	0.35 ± 0.03	0.51 ± 0.06

Figure 5 (a) and (b) illustrates the permeability curves of curcumin and resveratrol for Cur-Res suspension and Cur-Res gel, respectively. Those permeation profiles are biphasic in nature. The initial phase is characterized by relatively faster increase in permeability through 12 h period after which it is relatively slowed down and sustained. Such permeability profile can be due to various factors: i. The higher initial concentration gradient causing a greater Fickian diffusion, ii. Later on, the concentration gradient may decease resulting in corresponding slowing down of diffusion mediated permeation, iii. The skin condition might change with time as initially it was devoid of any bound drug but later on drugs got bound with it which could have slowed down the permeability, iv. The structural integrity of skin is more disrupted or loosened in the beginning by Cur-Res SLNs and other formulation components which could have been partially reversed later on, and v. The formulation excipients might have created additional transient channels in the skin allowing a greater permeation of drugs initially but later on at constant rate possibly due to gradual healing of such channels.

The cumulative amount of the drug permeated per unit area was plotted against time and the slope of the plot gave the

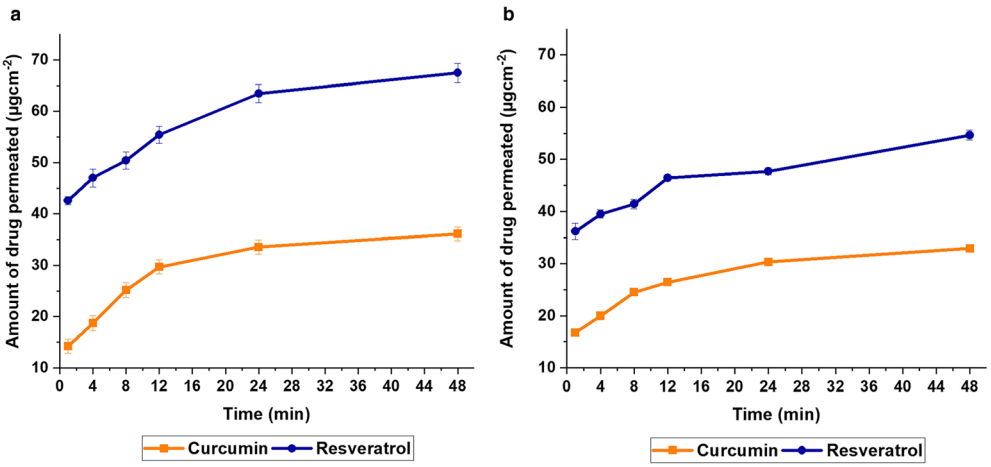

Fig. 5 Permeation of curcumin and resveratrol from Cur-Res SLNs (a) suspension (b) gel through shed snake skin for 48 h.

steady state flux (Table V). The steady state flux of curcumin was 0.31 ± 0.08 and 0.41 ± 0.01 μgcm^{-2} h^{-1} for Cur-Res gel and its suspension, respectively. It was 0.35 ± 0.03 and 0.51 ± 0.06 μgcm^{-2} h^{-1} for resveratrol from Cur-Res gel and its suspension, respectively. Results seem to indicate that Cur-Res SLNs (suspension) formulation allows for faster release of polyphenols in comparison to gel formulation. This might be due to entrapment of polyphenols in gel which required overcoming dual barriers provided by lipid and gel matrix whereas polyphenols loaded in SLNs (suspension) required overcoming only lipid matrix. Thus, it appears that the gel matrix acts as an additional rate-limiting barrier which can be easily manipulated to modulate flux.

Furthermore, a definitive conclusion couldn't be drawn based on the flux values since it depends on other factors like drug concentration, physical and chemical properties of drug such as solubility, molecular weight, pKa, structure, etc. (43). Therefore, further studies are required to study the correlation between drug permeation and these parameters.

The retention of curcumin and resveratrol in skin was further corroborated by the qualitative analysis of samples by ESI MS in Q_1 negative mode (data presented in supplemental Fig. 1) The curcumin and resveratrol peaks were found at m/z 337.1 and m/z 227.0 respectively.

Overall, it was clearly observed that the amount of curcumin from both formulations permeated and retained in the snake skin was considerably low compared to resveratrol from the respective formulations. This phenomenon can be due to the lipophilic nature of curcumin. Curcumin exhibits higher liposolubility compared to resveratrol resulting in stronger affinity to the lipid matrix of SLNs. Therefore, a higher amount of free resveratrol was available for skin penetration resulting in faster release of resveratrol. Friedrich et al. (25) reported similar results regarding the skin penetration of curcumin and resveratrol. Curcumin and resveratrol loaded lipid-core nanocapsules (RC-LNC) were formulated and analyze their skin penetration characteristics. The results indicated that the larger amount of resveratrol was found in all the skin layers (stratum corneum, viable epidermis and dermis) compared to curcumin due to the faster release profile of resveratrol from RC-LNC. Unfortunately, the release data and permeation data can't be correlated due to the limitation of these studies. Additional studies in future will be carried out to understand the release data of SLNs compared to pure drug solutions and to correlate the release date with the permeation data of SLNs.

Electrical Cell Substrate Impedance Sensing (ECIS)

The electrical cell-substrate impedance sensing (ECIS) device was invented by Giaever and Keese (27) to evaluate the morphological changes of adherent cells in a nanoscale range. Cell-cell and cell-matrix interactions (32), wound healing processes (77), cell proliferation, motility (48) and, signal transduction for modern drug discovery (75) are some of applications that can be assessed using ECIS. Impedance is a more general term for resistance. Impedance and resistance are both given in units of "ohms". Resistance is the opposition to a direct current (DC) which is independent of the frequency. However, impedance is a quantity used for the alternating current (AC). Since the electric current of the AC changes its direction periodically, other factors including inductance, capacitance are also considered when calculating impedance. Therefore, impedance is the total contribution of both resistance and reactance (39). The reactance is capacitive reactance where capacitance is involved. It is inductive reactance where inductance is involved. In the ECIS, there is capacitive reactance.

R = Resistance.

C = Capacitance.

f = Frequency of Ac current

$$z = \sqrt{R^2 + \left[\frac{1}{2\pi fC}\right]}$$

The cell membrane consists of a phospholipid bilayer which separates the ions and charged protein in the cytoplasm from the ions in the extracellular cells. Due to this characteristic of the cell membrane, both resistance and capacitance occur over the cell membrane. A mathematical approximation to determine the total impedance of cells covering electrode is given by the following equation.

It is found that cell-cell and cell-matrix interactions can be accurately measured when ECIS results are presented as the change in barrier resistance over time at high frequency (78). Capacitive reactance of the membrane is measured by $1/(2\pi fC)$; where f is the frequency and C is the capacitance. Therefore, capacitive reactance is inversely proportional to AC frequency. At higher frequency capacitive reactance of membrane is negligible, and the resistance alone adequately indicates the changes of cell seeding, attachment, migration, and proliferation.

In this study, B16F10 cell response to Cur-Res combination including Cur-Res SLNs, Cur-Res solution, curcumin solution, and resveratrol solution was studied by monitoring the resistance over 50 h. Figure 6 (a). given below show the ECIS results of two independent experiments that were conducted to test the effects on cell viability and motility with addition of Cur- Res and blank SLNs. The data were presented as the normalized resistance against time.

The initial normalized resistance (time 0 h) of the electrodes at 40 kHz ranges around 1 Ω. As shown in each graph, the resistance of B16F10 melanoma cells was observed to increase and fluctuate with time due to their rapid proliferation and spreading. These fluctuations are observed with all the other conditions that have been analysed with ECIS and are

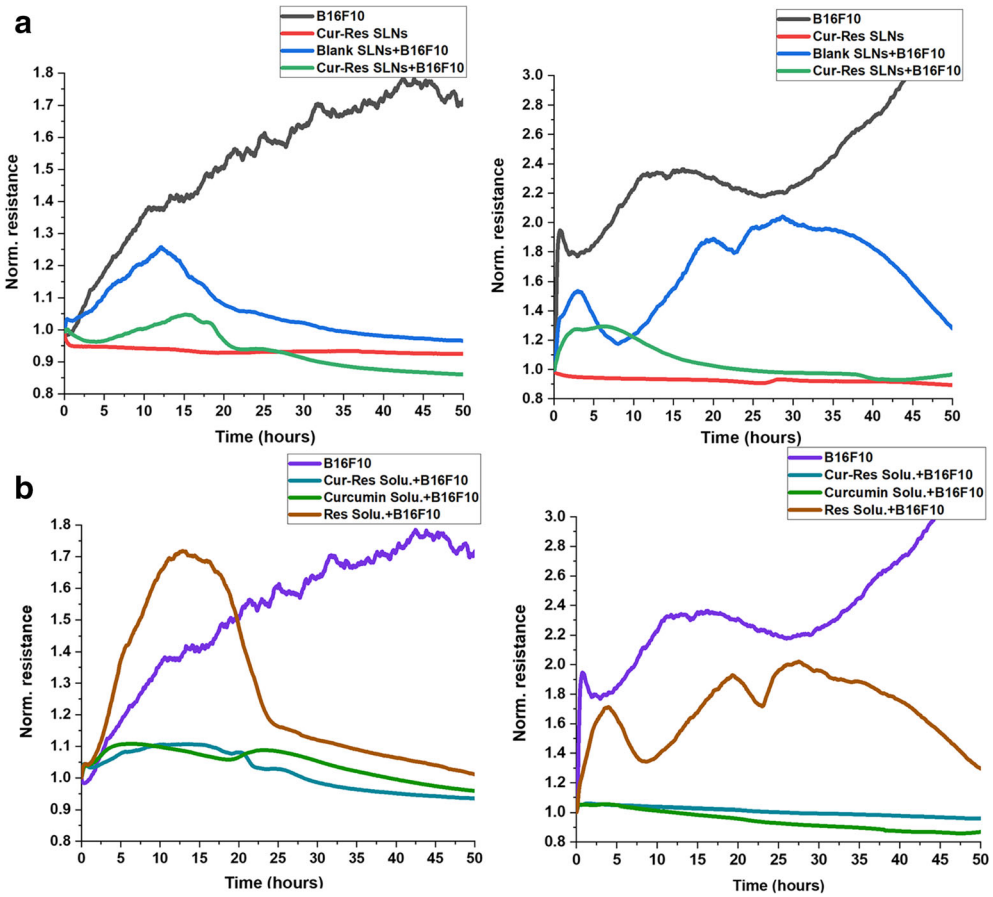

Fig. 6 (a) ECIS results for the B16F10 with addition of Cur-Res SLNs (Cur-Res; 60 + 20 μg/ml). B16F10 melanoma cell line, the cell free media and blank SLNs were used as controls; (b) ECIS analysis of the B16F10 with addition of Cur-Res solution (60 + 20 μg/ml), curcumin solution (60 μg/ml), and resveratrol solution (20 μg/ml). B16F10 melanoma cell line, was used as a control. Measurements were taken at multiple frequencies (100 Hz to 10,000 kHz) and the results for 40 kHz are shown here.

indicative of living cells and their movements on the electrodes (46, 54).

In the case of Cur-Res SLNs treated cells (Fig. 6 (a)), both $n = 1$ and $n = 2$ experiments showed the increase in resistance followed by a sudden drop. The increase of the resistance shows the migration of B16F10 cells and the sudden fall in resistance is assumed to be the response of cell death or detachment of cells from the substrate. Blank SLNs were used as control and the purpose of using blank SLNs is to prove that composition of lipid nanoparticles is non-toxic. In other words, toxic effects only come from the curcumin and resveratrol. The resistance of the cells exposed to blank SLNs increased over time except for n = 1 experiment. It may be due to some technical errors such as electrode damage. However, the increase of the resistance suggested that the composition of the SLNs such as lipid and surfactants are non-toxic to the melanoma cells. The resistance signal was monitored using cell-free electrode with Cur-Res SLNs to show that resistance is not influenced by Cur-Res SLNs when cells are absent. As shown in Fig. 6 (a), the resistance signal from Cur-Res SLNs without cells was a straight horizontal line.

Sambale et al. (63) conducted a similar study to investigate the toxic effects of silver nanoparticles on human lung adenocarcinoma epithelial cell line (A-549). Impedance measurements of A-549 were measured upon the addition of 10 ppm silver nanoparticles. Three conditions, including cell-free electrode with silver nanoparticles, cell-free electrode with medium and normal cell culture were used as a control. A drastic drop of the impedance was observed almost immediately after the addition of the silver nanoparticles indicating changes in cell morphology and attachment.

Two independent experiments were conducted to test the effects of melanoma cell growth in DMEM medium with the addition of Cur-Res solution, curcumin solution, and resveratrol solution (Fig. 6 (b)). The initial resistance of the electrodes in all two experiments ranges around 1 **Ω**. As shown in each graph, the resistance of B16F10 melanoma cells gradually increased with time because the cells were live, and they were rapidly proliferating and attaching to electrodes. It is observed that resveratrol did not show significant growth inhibition on B16F10 compared to curcumin solution (60 μg/ml). The resistance steadily increased with cells exposed to resveratrol as a result of cell adhesion and spread over the electrodes. This may be due to low resveratrol concentration. There is no significant difference in the resistance between curcumin and Cur-Res solution. Both curves of curcumin solution and Cur-Res solution trend downwards. This is assumed to be the

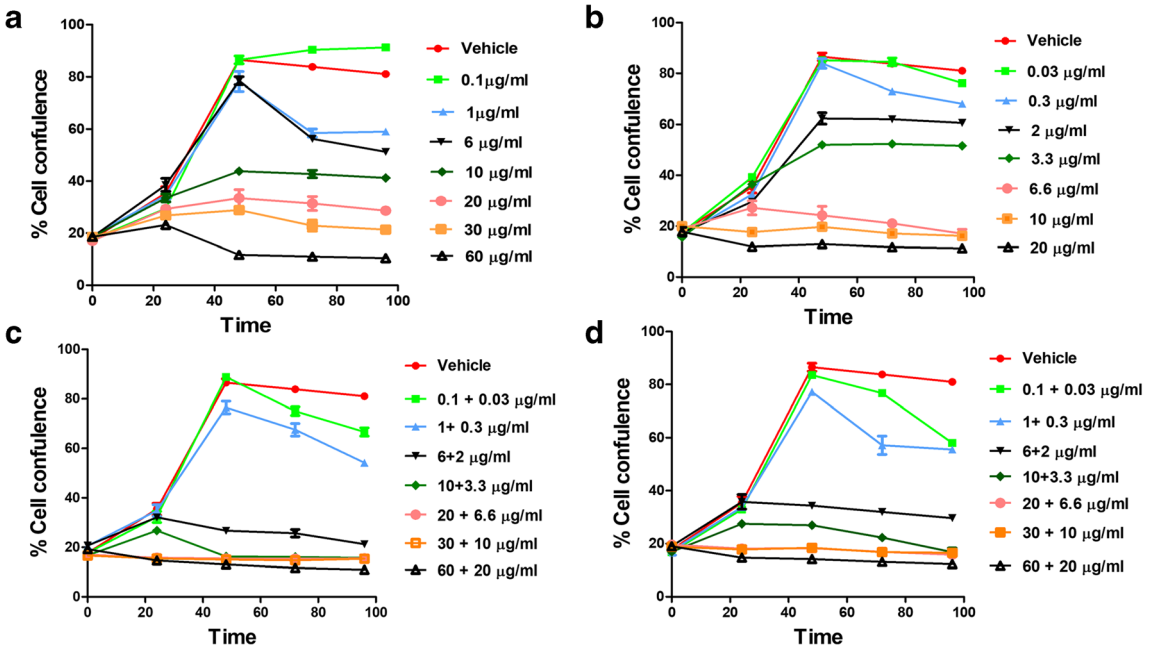

Fig. 7 Effect of (a) curcumin, (b) resveratrol, (c) Cur-Res solution, (d) Cur-Res SLNs on SK-MEL-28 cell confluence percentage over time. Cells were incubated with seven different concentrations ranging from 0.1 µg/ml-60 µg/ml, 0.03–20 µg/ml, and 0.1 + 0.03 to 60–20 µg/ml, respectively over a 96 h period. Cell confluence percentage was analysed every 24 h using. IncuCyte instrument. Values represent the mean ± standard deviations of three independent experiments.

response of cell death including detachment of cells from the substrate.

Analysis of Molecular Activity between Curcumin and Resveratrol

IncuCyte Cell Proliferation Assay

The IncuCyte® live cell analysis system provides the real-time automated measurements of cell growth and inhibition via monitoring the cell confluence under treatment ((40). The endpoint cell viability assay was also performed after 96 h to ensure that the changes of SK-MEL-28 cell confluence were happened because of the reduction of cancer cell viability (41, 71). The human melanoma cell line (SK-MEL-28) which is derived from an axillary lymph node of 51-year-old male was utilized as an experimental model to conduct this study. Figure 7 demonstrates the activity of curcumin, resveratrol, Cur-Res solution and Cur-Res SLNs on the cell proliferation of SK-MEL-28 melanoma cell lines.

The activity of the curcumin on the cell proliferation of SK-MEL-28 was tested using different curcumin concentrations range from 0.1–60 µg/ml for 96 h. No growth inhibition of cells was observed when cells were treated with DMSO (0.1%). When cells were monitored by the IncuCyte® live-cell analysis system, a significant reduction in cell confluence was found at 20, 30, and 60 µg/ml concentrations compared to the control.

The activity of the curcumin on the cell proliferation of SK-MEL-28 was tested using different curcumin concentrations range from 0.1–60 µg/ml for 96 h (Fig. 7 (a)). No growth inhibition of cells was observed when cells were treated with DMSO (0.1% *v*/v) which was used as control. When cells were monitored by the IncuCyte® live-cell analysis system, a significant reduction in cell confluence was found at 20, 30, and 60 µg/ml curcumin concentrations compared to the control. Approximately 81% of confluence was achieved when treated with DMSO (0.1% *w*/*v*), which was reduced to 10.43% when cells were treated with the 60 µg/ml of curcumin. There is a significant difference ($P < 0.001$) between curcumin concentration (60 µg/ml) and control. A similar pattern of growth inhibition was found between 20 and 30 µg/ml curcumin concentrations. The cell confluence was gradually increased until 48 h (28–33%), and then no significant increase in confluence was observed until 96 h. There was a statistically significant difference ($P < 0.001$) between control and aforementioned two concentrations. Furthermore, significant growth inhibition was observed after 96 h when cells were treated 10 µg/ml of curcumin ($P < 0.001$). Both 1 ($P < 0.01$) and 6 ($P < 0.06$) µg/ml curcumin concentrations have shown a notable growth inhibition on SK-MEL-28 and reduced the cell confluence respectively to 59 and 51%. The cell confluence was gradually increased when cells were treated with 0.1 µg/ml of curcumin. It was too low to show the significant growth inhibition on the SK-MEL-28 cell line. Figure 7 (b) demonstrates the activity of the resveratrol on the cell proliferation of SK-MEL-28, which

was tested using seven different concentrations range from 0.03–20 μg/ml for 96 h. As shown in Fig. 7 (b), vehicle (DMSO 0.1% *v*/v) was found to be non-toxic against the melanoma cell line, and cell confluence was 81% ± 0.56 after 96 h. The graph depicts the significant percent change in confluence between 20 μg/ml resveratrol concentration (11. 25% ± 1.06) and the control after 96 h. A significant difference between control and highest resveratrol concentration (20 μg/ml) is indicated by $P < 0.001$. Similar trend of growth inhibition was observed in both 6.6 and 10 μg/ml resveratrol concentrations. The initial confluence for both these concentrations was found to be 20%, and as the result of the anticancer activity of the resveratrol, the cell confluence was decreased to 17% after 96 h for both resveratrol concentrations (6.6 and 10 μg/ml). There was a statistically significant difference ($P < 0.001$) between the control and the aforementioned two concentrations. Resveratrol was shown to suppress the confluence at 3.3 and 2 μg/ml. After 96 h, both these concentrations showed a statistically significant difference; $P < 0.001$ and $P < 0.01$ respectively compared to control. Approximately 76% ± 1.2 of cells remained viable when treated with 0.03 μg/ml of resveratrol, which was reduced to 68.15% ± 0.49 when cells were treated with 0.3 μg/ml of resveratrol, which makes only a $P < 0.05$ statistical significance between 0.03 and 0.3 μg/ml. However, these two concentrations were too low to have a significant growth inhibition on SK-MEL-28 as compared to 20 μg/ml.

The activity of the combination of curcumin and resveratrol on the cell proliferation of SK-MEL-28 was tested using seven Cur-Res combinations ranging from 0.1+ 0.03 to 60 + 20 μg/ml for 96 h (Fig. 7 (c)). IncuCyte data showed that there is no growth inhibition was observed at DMSO 0.1% *v*/v; approximately 81% ± 0.56 of cells remained viable after 96 h. However, 60 + 20 μg/ml Cur-Res combination has shown a significant growth inhibition on SK-MEL-28 and reduced the cell confluence to 10.98% ± 1.10. The similar observations were reported on the effects of 30 + 10, 20 + 6.6, and 10 + 3.3 μg/ml Cur-Res combinations on the proliferation of SK-MEL-28 cells. The initial cell confluence for all the three drug combinations was found to be 16%, and it decreased to 15% at the end of 96 h. Furthermore, significant growth inhibition was observed after 96 h when cells were treated 6 + 0.2 μg/ml Cur-Res combination. All the Cur-Res combinations except 0.1 + 0.03 and 1 + 0.03 μg/ml showed a statistically significant difference; $P < 0.001$ compared to control. The similar trend was observed in cell confluence for both 0.1 + 0.03 ($P < 0.05$) and 1 + 0.03 ($P < 0.01$) μg/ml Cur-Res combinations over time. The amount curcumin and resveratrol in 0.1 + 0.03 and 1 + 0.03 drug combinations was low compared to other drug combinations to show a noticeable reduction in cell proliferation.

The IncuCyte assay monitored the anticancer activity of both curcumin and resveratrol in solid lipid nanoparticles on cell proliferation of SK-MEL-28 (Fig. 7 (b)). Blank SLNs (vehicle) was used as the control and shown to have an insignificant effect on a cell proliferation resulting in 82% ± 0.09 of cell confluence was achieved after 96 h. However, IncuCyte cell proliferation assay showed the significant growth inhibition of melanoma cell lined when treated with 60 + 20 μg/ml Cur-Res combination up to 96 h compared to blank nanoparticles ($P < 0.001$). The similar observations were reported on the effects of 30 + 10, and 20 + 6.6 μg/ml Cur-Res combinations on the proliferation of SK-MEL-28 cells. The initial cell confluence was found to be around 19%, and it decreased to 16% at the end of 96 h. The 10 + 3.3 μg/ml Cur-Res combination also showed an increase in cell confluence until 48 h then followed by a drastic reduction in cell confluency. In addition, the cell confluence was gradually increased to 35.75 ± 0.72 and then decreased to 29.61 ± 0.72 at the end of 96 h when cells were treated with 6 + 2 μg/ml. There is a statistically significant difference ($P < 0.001$) between control and Cur-Res combinations, including 30 + 10, 20 + 6.6, 10 + 3.3, and 6 + 2 μg/ml. Both 1 + 0.3 and 0.1 + 0.03 Cur-Res combinations showed noticeable inhibition effects on SK-MEL-28 cell proliferation after 48 h. Both combinations drastically decreased the cell confluence from 80% to 56% after 48 h.

Figure 8 (a) and (b) demonstrates the cell viability of SK-MEL-28 cells treated with curcumin and resveratrol solutions at 96 h. As expected, the cell viability of curcumin and resveratrol was concentration- and time- dependent. The cell viability decreased with increased concentrations in SK-MEL-28 cell line. A notable growth inhibition ($P < 0.01$) was observed above 1 and 0.3 μg/ml for free curcumin and resveratrol respectively. However, Cur-Res solution was found to be more toxic than either drug solution alone. In this study, Cur-Res solution was shown to suppress cell confluence to less than 20% and induce cell death at Cur-Res concentrations above 6 + 2 μg/ml ($P < 0.001$) whereas only highest curcumin (30 and 60 μg/ml; $P < 0.001$) and resveratrol (6.6, 10 and 20 μg/ml; $P < 0.001$) concentrations exhibited significant growth inhibition (< 20%). This can be due to the synergistic activity of curcumin and resveratrol

One of the major issues associated with nanoparticles is toxicity. Nanoparticles can pose adverse side effects due to their characteristics, including high surface activity, small diameter, high surface area, unusual morphologies (61). As shown in Fig. 7, blank SLNs data reveal that they have no cytotoxic effects on cell proliferation as the cellular viability was above 80% at all concentrations after 48 h. It indicates that the noticeable cytotoxic effects of Cur-Res SLNs were solely due to the anticancer activity of curcumin and resveratrol. On the other hand, Cur-Res SLNs significantly reduced the cell viability in a concentration- and time- dependent manner. The cells exposed to 0.1 + 0.03 and 6 + 2 μg/ml Cur-Res SLNs showed approximately 56.8 and 29.1%

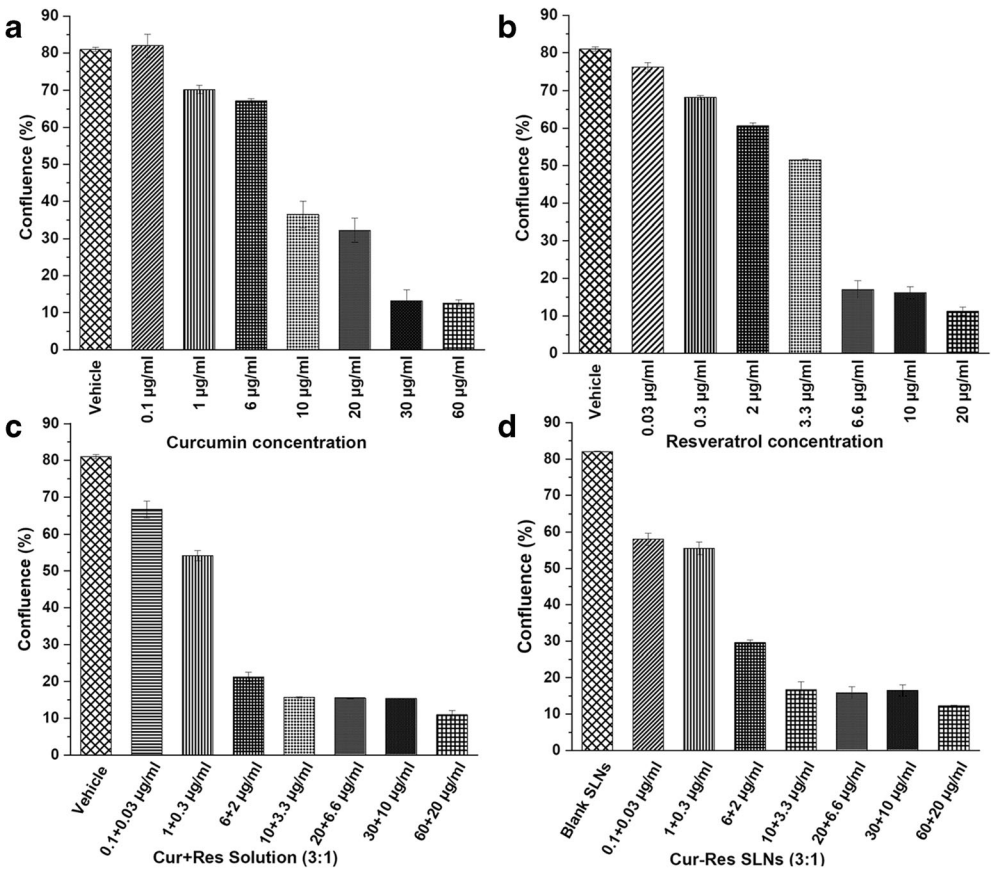

Fig. 8 Effects of (a) curcumin solution, (b) resveratrol solution, (c) Cur-Res solution, and (d) Cur-Res SLNs on SK-MEL-28cell confluence at 96 h. Values represent the mean ± standard deviations of two independent experiments (Significant: *$P < 0.05$, **$0.01 < P$, ***$P < 0.001$ and non-significant (n.s).

viability, respectively after 96 h. Treatment with 10 + 3.3 µg/ml Cur-Res SLNs decreased the cell viability to 15.23%. Viability of cells treated with 60 + 20 further reduced to 10.29%. Overall, Cur-Res SLNs showed a significant difference ($P < 0.001$) above 6 + 2 µg/ml in growth inhibition compared to cells exposed to blank SLNs.

A limited number of studies have been focused on the mechanism of action of solid lipid nanoparticles. Solid lipid nanoparticle can enter the cell via three possible mechanisms including penetration, adhesion and/or fusion. Nanoparticles can be taken up by cells if they are small enough. Furthermore, particles can release drug into the cell by either adhesion on to the surface of the cell membrane, or fusion and mixing with intracellular lipids, resulting in significant drug penetration through cell membrane (2).

Table VI IC_{50} values for curcumin, resveratrol and combination of Cur-Res (3:1) in solution and SLNs

Drug/ Combination	IC_{50} (µg/ml)	Mean ± SD
Curcumin	6.38	0.275
Resveratrol	3.67	0.14
Cur-Res Sol.	1.8	0.07
Cur-Res SLNs	1.6	0.09

The aim of this present study to compare the cytotoxic effects between Cur-Res SLNs and Cur-Res solution, on SK-MEL-28 cell line. As shown in Fig. 8 (c) and (d), there was no significant difference in cell viability and cell proliferation between Cur-Res solution and Cur-Res SLNs. Both showed higher toxicity to SK-MEL-28 when compared to DMSO (0.1% *v*/v) and Blank SLNs. Like Cur-Res SLNs, Cur-Res solution decreased cell viability in a concentration- and time- dependent manner. With the Cur-Res concentration of solution increasing from 0.1 + 0.03 µg/ml to 60 + 20 µg/ml, the relative cell viability of SK-MEL-28 decreased from 68.3 to 10.2% at 96 h. Tested the cytotoxicity of curcumin loaded mPEG-PLA-Ch micelles and curcumin solution on B16F10 cell line. The similar toxic profile was observed for both treatments after 24 h. Both free curcumin and curcumin loaded mPEG-PLA-Ch significantly reduced cell viability in a concentration-dependent. However, no significance in difference in cell viability was observed between free curcumin solution and curcumin loaded mPEG-PLA-Ch.

Carletto et al. (11) developed Poly(ε-caprolactone) loaded with resveratrol. The formulation was tested for cytotoxicity on B16F10 cell line. The results indicated that cell viability

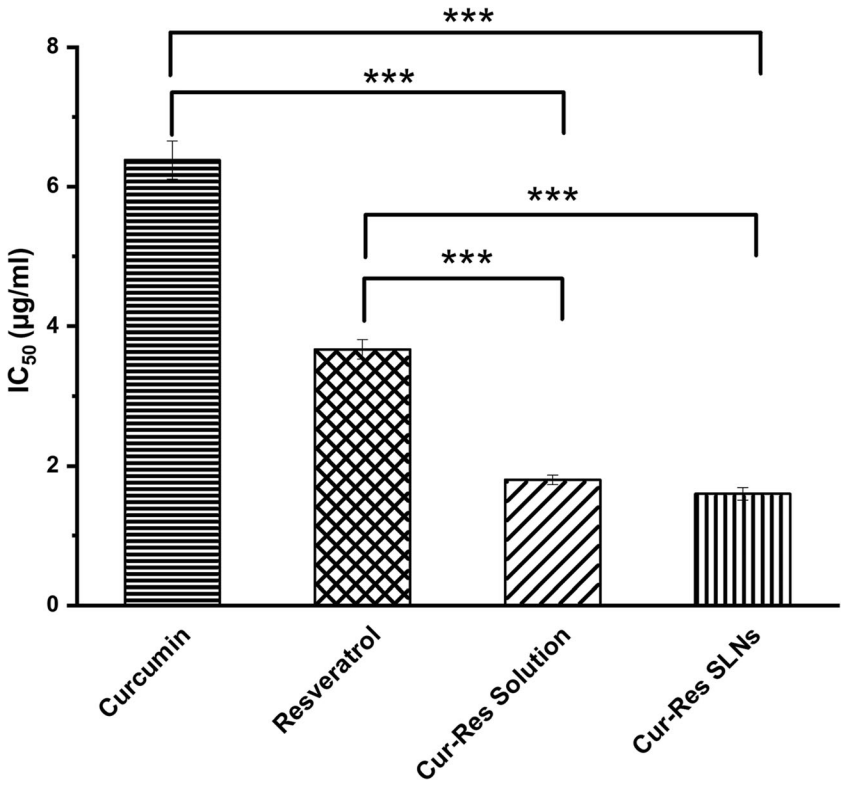

Fig. 9 In vitro cytotoxicity plots of curcumin, resveratrol, Cur-Res (3:1) solution and SLNs ($n = 6$). ***$P < 0.001$ indicates the statistically significant difference between single polyphenol and Cur-Res combinations.

was concentration-dependent with viability decreasing with increased concentrations for both free resveratrol and resveratrol loaded nanoparticles (Res-NP). Both the treatments showed higher toxicity at higher concentrations (100 and 300 M). Furthermore, no statistical difference was observed in cell viability between resveratrol and Res-NP indicating that resveratrol loaded nanoparticles can be used as a feasible approach to deliver drugs.

MTT assay was conducted to study the cytotoxicity against SK-MEL-28 cell line in a concentration-dependent manner for curcumin and resveratrol individually and combination. Anticancer properties of Cur-Res 3:1 combination was investigated using two systems; Cur-Res solution and Cur-Res SLNs. Free curcumin and resveratrol were used as controls. Based on the previous studies by other groups, 3:1 Cur-Res combination was utilized to assess the cell viability in this study. Pushpalatha et al. (59) investigated the cytotoxicity effects of curcumin and resveratrol individually and 3:1, 1:1, 1:3 Cur-Res combination against human breast cancer MCF-7 cell line. It is evident from the results that the IC_{50} value observed for curcumin and resveratrol was 21.29 µg/ml, and 38.30 µg/ml. However, 3:1 Cur-Res combination enhanced the growth inhibition significantly with having the lowest half maximal inhibitory concentration (IC_{50}) value of 8.29 µg/ml.

Table VI and Fig. 9 show the (IC_{50}) values of Cur-Res solution and SLNs in comparison to free curcumin and resveratrol controls. As demonstrated in Table VI, IC_{50} dosage for curcumin after 96 h was 6.38 µg/ml and for the resveratrol was 3.67 µg/ml. However, the Cur-Res solution and SLNs significantly reduced the IC_{50} dosage when compared to curcumin and resveratrol alone. The IC_{50} dosage for the combination of Cur-Res solution and SLNs were 1.8 µg/ml and 1.6 µg/ml respectively, which indicated statistically significant difference compared to either agent alone ($P < 0.001$). However, no statistical difference was observed in IC_{50} dosages between Cur-Res solution and SLNs.

According to the study finding, resveratrol showed greater cytotoxic effects on human melanoma (SK-MEL-28) (IC_{50} = 3.67 µg/ml after 96 h; $P < 0.001$) compared to curcumin (IC_{50} = 6.38 µg/ml after 96 h; $P < 0.001$). Inhibitory effects of resveratrol (10, 50, and 100 µM) on human melanoma cell line (SK-MEL-31) were investigated by Wu et al. (85). The IC_{50} value for resveratrol found to be 15 µM (5.527 µg/ml) after 48 h. Similar findings were observed in the study of Fuggetta et al. (26). The results demonstrated that resveratrol significantly inhibited the proliferation of SK-MEL-28 with IC_{50} value of 8 ± 1.4 µg/ml after 5 days.

A number of studies have been conducted to understand the molecular activity of curcumin on melanoma cell lines (SK-MEL-28, B16F10, A375) in comparison to curcumin

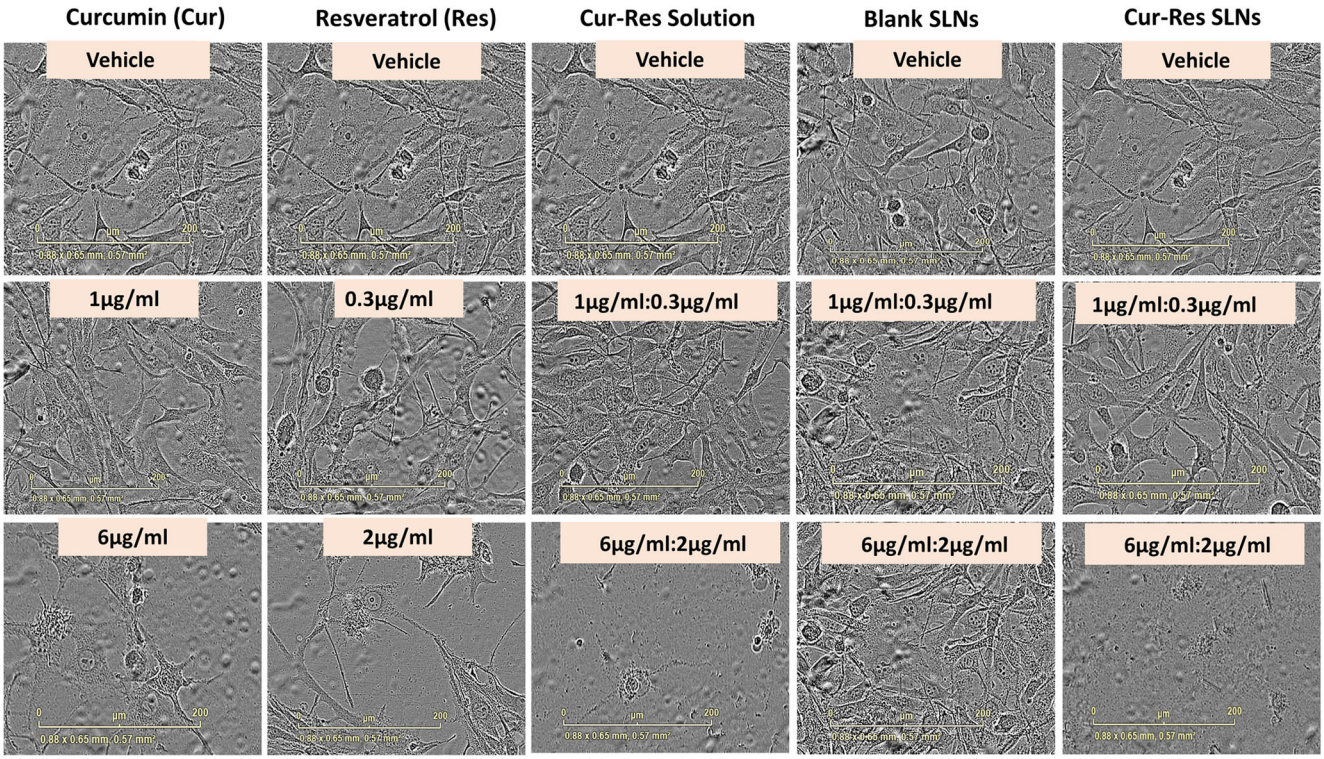

Fig. 10 Morphological changes in SK-MEL-28 human melanoma cells treated with Curcumin (Cur, 1, and 6 μg/ml), Resveratrol (Res 0.3, and 2 μg/ml), Cur-Res combination in solution and loaded in SLNs with a ratio of 3:1.

loaded nanoparticles. Some studies reported that IC_{50} value was not reduced when using curcumin loaded nanoparticles compared to free curcumin. In Anuchapreeda et al. (6) study, IC_{50} value for the free curcumin and curcumin loaded nanoemulsion found about 3.5 ± 0.5 and 22.2 ± 0.6 µM against B16F10 respectively. Curcumin loaded nanoemulsion

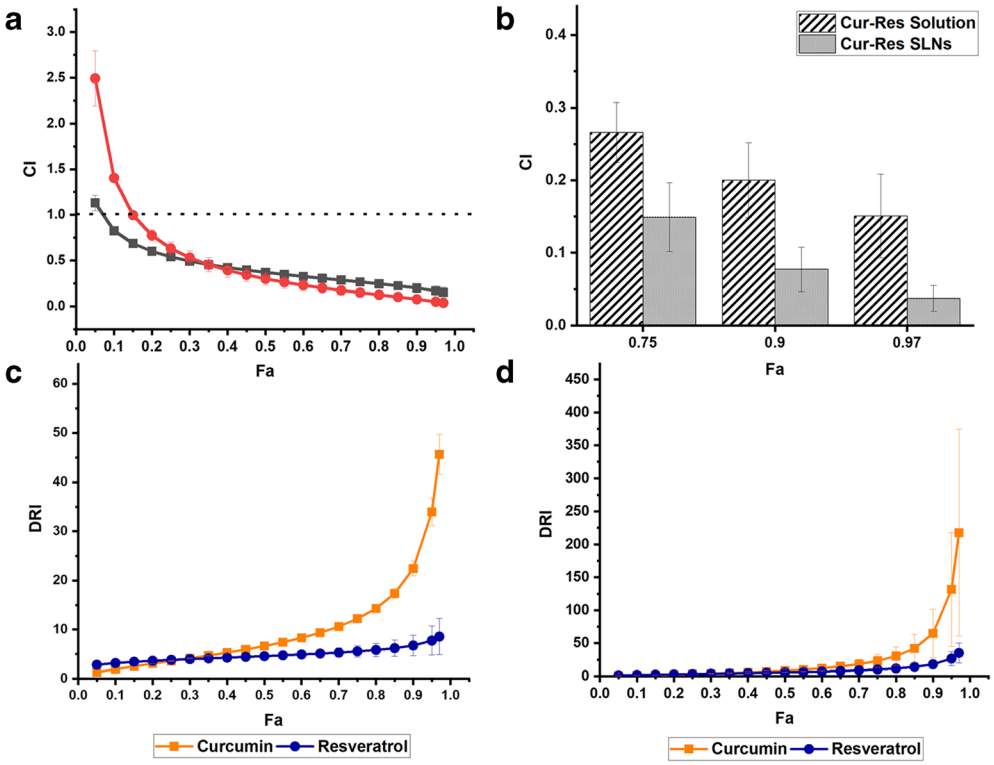

Fig. 11 (a) the graphic summary of CI analysis at overall levels of effect (Fa) ranging from 0.5 to 0.97; (b) highlighted the CI computed at higher cell lethality (Fa > 0.5); ED 75, ED 90, and ED 95; (c) Fa-DRI plots for Cur-Res solution; (d) Fa-DRI plots for Cur-Res SLNs.

showed lower cytotoxic effects and the difference is statistically significant compared to free curcumin. The result is in parallel to the cytotoxicity effects of curcumin loaded chitosan-coated polycaprolactone nanoparticles in B16F10 cell line with the IC_{50} value of 119.3 ± 2.35 μM after 24 h (47). Mazzarino et al. (50) observed the similar results where IC_{50} values of curcumin loaded nanoparticles were significantly higher than free curcumin for all exposure times. This might be due to uncompleted drug release from a nanoparticle which results in the less availability of the curcumin in the culture media. However, previous studies by other groups indicated that IC_{50} value depends on the several parameters, including time, cell line, physical conditions of the experiment (84). For an example, Wang et al. (81) demonstrated that IC_{50} value for curcumin loaded MPEG-PLA micelles (A375: 8.3 μg/ml; B16F10: 8.9 μg/ml) was lower than free curcumin (A375 12.5 μg/ml; B16F10: 9.8 μg/ml) after 24 h.

Statistically significant reduction of IC_{50} values was seen after treatment with Cur-Res solution and SLNs compared to single agents. This may be due to the synergistic activity of curcumin and resveratrol (49, 60). However, no significant difference was observed between the growth inhibitory effects of Cur-Res solution and Cur-Res SLNs. Nevertheless, Cur-Res SLNs showed slightly lower IC_{50} value (1.6 μg/ml) compared to Cur-Res solution (1.8 μg/ml). This is possibly due to enhanced solubility and stability of the drugs in the SLNs. Another possible reason could be nanoscale particle size resulted in greater uptake of the compounds at the intracellular level (82). Similar results were reported by Pushpalatha, Selvamuthukumar, and Kilimozhi (60) where they have shown that 3:1 curcumin and resveratrol loaded cyclodextrin nanosponge (Cur-Res CDNS) has lowest IC_{50} value (3.41 μg/ml) compared to 1:1 (9.84 μg/ml) and 1:3 (14.98 μg/ml) Cur-Res CDNS after 72 h.

Morphology Analysis

Figure 10 demonstrates the changes in cellular morphology of SK-MEL-28 cells. It can be seen that after 96 h, a number of viable cells in cell layer were gradually decreasing with increase in concentrations of Cur Sol., Res Sol., Cur-Res Sol. and Cur-Res SLNs compared to controls. However, significant cell death was observed in the wells treated with 6 + 2 μg/ml of Cur-Res combinations in solution and loaded SLNs compared to Cur and Res alone. Cell density was decreased and the size of most cells in the 6 + 2 μg/ml Cur-Res treated groups (Cur-Res solution and Cur-Res SLNs) was shrunk compared with curcumin and resveratrol alone.

Combination Index and Dose Reduction Index

The purpose of combination therapy is to reduce side effects and cost, increase chemopreventive effectiveness, synergistic effects, and increase compliance (69). To our knowledge, this is the first time that a synergistic effect of the combination of curcumin and resveratrol in SK-MEL-28 melanoma cell line have been quantitatively determined.

As shown in Fig. 11 (a), synergistic effects were recorded at all the dose levels except Fa = 0.05 for both Cur-Res solution and SLNs. CI values of Cur-Res SLNs were below 0.2 at the effect level greater than 75% inhibition. Similarly, CI values of Cur-Res solution at ED 75, ED 90 and ED 95 were 0.25, 0.2 and 0.15. A general trend of increasing synergistic effects for both Cur-Res solution. and SLNs was evidenced with the increase in levels of cancer cell inhibition. However, synergism with high effect levels (ED 75, ED 90, ED 95) is much more therapeutical important in the cancer treatment when compared to low effect levels (< ED 50) (14). For both Cur-Res solution and SLNs, highest synergism was shown by curcumin with resveratrol at ED 95 followed by ED 90 and ED 75 (Fig. 11 (b)). However, Cur-Res SLNs produced stronger synergistic effects compared to Cur-Res solution at high effect levels. This might be because Cur-Res SLNs efficiently deliver both curcumin and resveratrol into a cell when compared to Cur-Res solution. A number of studies against different cancer cell lines demonstrated that curcumin in combination with resveratrol was more effective than either agent alone in inhibiting tumour growth. Another study using colon cancer HCT-116 cells reported that curcumin synergizes with resveratrol to inhibit cell proliferation (49). Du et al. (20) conducted a similar study indicating that curcumin and resveratrol combination significantly inhibit the tumour growth of hepatocellular carcinoma Hepa1–6 growth when compared to either agent alone.

Figure 11 (c) and (d) demonstrates the Fa-DRI plots for Cur-Res solution and SLNs. Both formulations exhibited the DRI larger than 1 for curcumin and resveratrol indicating favourable dose reduction. However, the dose reduction index for curcumin and resveratrol in SLNs was much higher at higher Fa levels (0.5 > Fa) compared to the solution. The major barrier to these polyphenol's clinical efficacy is their poor bioavailability. The advantage of the dose reduction is, less concentration of respective polyphenols is required on the site of action to give the same efficacy compared to polyphenol alone. Therefore, it is important to realize that lower in vitro concentration of curcumin and resveratrol is more achievable in vivo. Recently, Ediriwickrema et al. (21) have formulated multilayered nanoparticles (CT MLNPs) for co-delivery of camptothecin (CPT) and plasmid encoding TNF related apoptosis inducing ligand (pTRAIL) and evaluated the ability of nanoparticle to inhibit the tumor growth through synergistic activity of CPT and pTRAIL using three different cell lines; HCT116, U87, and MDAMB231. The results indicated that CT MLNP produced IC50 values with DRI ranging from 4.66 to 7.99 for pTRAIL and 3.14 to 14.5 for CPT.

CONCLUSION

In conclusion, solid lipid nanoparticles were successfully fabricated using Compritol 888 ATO as solid lipid and loaded with curcumin and resveratrol. These nanosized Cur-Res SLNs demonstrated higher encapsulation efficiency and skin binding. Furthermore, newly developed Cur-Res SLNs found to be physically stable at 4°C with respect to particle size lower than 300 nm over a period of 3 weeks. The in vitro release study showed a greater release profile for resveratrol compared to curcumin. The Slide-A-Lyzer Dialysis Cassettes were used to conduct the in vitro studies and results showed that the release profile of curcumin was significantly low compared to resveratrol. The inhibitory effects of Cur-Res SLNs on melanoma cell proliferation were studied using ECIS (Electrical cell substrate impedance method). The results from ECIS measurements indicated that both Cur-Res solution and Cur-Res SLNs have potential to stop cell migration of B16F10 melanoma cells. The synergism in anticancer effects of curcumin and resveratrol toward SK-MEL-28 cell was evaluated by using Cur-Res SLNs and Cur-Res solution. IncuCyte cell proliferation assay showed that both Cur-Res SLN and Cur-res solution. Significantly reduced the cell viability in a concentration- and time-dependent manner. Blank SLNs did not show any cytotoxic effects on cell proliferation, which indicating noticeable cytotoxic effects of Cur-Res SLNs were solely due to the anticancer activity of curcumin and resveratrol. MTT results showed that the combination of curcumin and resveratrol in solution and SLNs significantly reduced the IC50 dosage when compared to curcumin and resveratrol alone ($P < 0.001$). The combination of curcumin and resveratrol proved to be synergistic at all the dose levels. DRI data demonstrated that the combination of Cur-Res showed a favorable dose reduction for both curcumin and resveratrol. In the light of these results, solid lipid nanoparticles are ideal carrier systems for the delivery of poorly soluble compounds including curcumin, resveratrol for topical administration.

SUPPLEMENTARY INFORMATION

The online version contains supplementary material available at https://doi.org/10.1007/s11095-021-03043-7.

REFERENCES

1. Aburahma M, Badr-Eldin S. Compritol 888 ATO: a multifunctional lipid excipient in drug delivery systems and nanopharmaceuticals. Expert Opinion on Drug Delivery. 2014;11(12):1865–83.
2. Akhtar N. Vesicles: a recently developed novel carrier for enhanced topical drug delivery. Current Drug Delivery. 2014;11(1):87–97.
3. Albash R, Abdelbary AA, Refai H, El-Nabarawi MA. Use of transethosomes for enhancing the transdermal delivery of olmesartan medoxomil: *in vitro*, ex vivo, and *in vivo* evaluation. Int J Nanomedicine. 2019;14:1953–68. https://doi.org/10.2147/IJN.S196771.
4. American cancer society. (2019). Key statistics for melanoma skin cancer. Retrieved 03/10, 2018, from https://www.cancer.org/cancer/melanoma-skin-cancer/about/key-statistics.html.
5. Ansari K, Vavia P, Trotta F, Cavalli R. Cyclodextrin-based nanosponges for delivery of resveratrol: *In vitro* characterisation, stability, cytotoxicity and permeation study. AAPS PharmSciTech. 2011;12(1):279–86.
6. Anuchapreeda S, Fukumori Y, Okonogi S, Ichikawa H. Preparation of lipid nanoemulsions incorporating curcumin for cancer therapy. Journal of Nanotechnology. 2012;2012:1–11.
7. Bhardwaj A, Sethi G, Vadhan-Raj S, Bueso-Ramos C, Takada Y, Gaur U, et al. Resveratrol inhibits proliferation, induces apoptosis, and overcomes chemoresistance through down-regulation of STAT3 and nuclear factor regulated antiapoptotic and cell survival gene products in human multiple myeloma cells. Blood. 2007;109(6):2293–302.
8. Bhatia, S., Tykodi, S. S., & Thompson, J. A. (2009). Treatment of metastatic melanoma: An overview. Oncology (Williston Park, N.Y.), 23(6), 488–496.
9. Bhatt P, Lalani R, Vhora I, Patil S, Amrutiya J, Misra A, et al. Liposomes encapsulating native and cyclodextrin enclosed paclitaxel: enhanced loading efficiency and its pharmacokinetic evaluation. Int J Pharm. 2018;536(1):95–107. https://doi.org/10.1016/j.ijpharm.2017.11.048.
10. Brubach JB, Jannin V, Mahler B, Bourgaux C, Lessieur P, Roy P, et al. Structural and thermal characterization of glyceryl behenate by X-ray diffraction coupled to differential calorimetry and infrared spectroscopy. Int J Pharm. 2007;336(2):248–56.
11. Carletto, B., Berton, J., Ferreira, T. N., Dalmolin, L. F., Paludo, K. S., Mainardes, R. M., et al. (2016). Resveratrol-loaded nanocapsules inhibit murine melanoma tumor growth doi: https://doi.org/10.1016/j.colsurfb.2016.04.001.
12. Chen J, Li L, Su J, Li B, Chen T, Wong Y. Synergistic apoptosis-inducing effects on A375 human melanoma cells of natural borneol and curcumin. PLoS One. 2014;9(6):e101277.
13. Chen Y, Wu Q, Zhang Z, Yuan L, Liu X, Zhou L. Preparation of curcumin-loaded liposomes and evaluation of their skin permeation and pharmacodynamics. Molecules (Basel, Switzerland). 2012;17(5):5972–87.
14. Chou, T. (2006). In Chou T. (Ed.), *Theoretical basis, experimental design, and computerized simulation of synergism and antagonism in drug combination studies*.
15. Coradini K, Lima FO, Oliveira CM, Chaves PS, Athayde ML, Carvalho LM, et al. Co-encapsulation of resveratrol and curcumin in lipid-core nanocapsules improves their *in vitro* antioxidant effects. Eur J Pharm Biopharm. 2014;88(1):178–85.
16. Danaei M, Dehghankhold M, Ataei S, Hasanzadeh Davarani F, Javanmard R, Dokhani A, et al. Impact of particle size and Polydispersity index on the clinical applications of Lipidic Nanocarrier systems. Pharmaceutics. 2018;10(2):57. https://doi.org/10.3390/pharmaceutics10020057.
17. Das RK, Kasoju N, Bora U. Encapsulation of curcumin in alginate-chitosan-pluronic composite nanoparticles for delivery to cancer cells. Nanomedicine. 2010;6(1):153–60.
18. Desai, P., Patlolla, R. R., & Singh, M. (2010). Interaction of nanoparticles and cell-penetrating peptides with skin for transdermal drug delivery. Molecular membrane biology, 2010, 27; Vol.27(7; 7), 247; 247-259; 259.
19. Deshpande, A. A. (2015). Formulation, characterization and evaluation of paclitaxel loaded solid lipid nanoparticles prepared by temperature modulated solidification technique. (Master of Science, The University of Toledo).

20. Du Q, Hu B, An H, Shen K, Xu L, Deng, S. And Wei, M. Synergistic anticancer effects of curcumin and resveratrol in Hepa1-6 hepatocellular carcinoma cells. Oncol Rep. 2013;29(5): 1851–8.
21. Ediriwickrema A, Zhou J, Deng Y, Saltzman W. Multi-layered nanoparticles for combination gene and drug delivery to tumors. Biomaterials. 2014;35(34):9343–54.
22. El-Housiny S, Shams Eldeen MA, El-Attar Y, Salem HA, Attia D, Bendas ER, et al. Fluconazole-loaded solid lipid nanoparticles topical gel for treatment of pityriasis versicolor: formulation and clinical study. Drug Delivery. 2018;25(1):78–90.
23. Freitas C, Müller RH. Effect of light and temperature on zeta potential and physical stability in solid lipid nanoparticle (SLN™) dispersions. Int J Pharm. 1998;168(2):221–9.
24. Freitas C, Müller RH. Correlation between long-term stability of solid lipid nanoparticles (SLN™) and crystallinity of the lipid phase. Eur J Pharm Biopharm. 1999;47(2):125–32. https://doi.org/10.1016/S0939-6411(98)00074-5.
25. Friedrich, R. B., Kann, B., Coradini, K., Offerhaus, H. L., Beck, R. C. R., & Windbergs, M. (2015). Skin penetration behavior of lipid-core nanocapsules for simultaneous delivery of resveratrol and curcumin. European journal of pharmaceutical sciences, 78, 204-213. 117.
26. Fuggetta P, Maria D'a P, Stefania L, Giulia P, Tricarico PM, Cannavò P, et al. *In vitro* antitumour activity of resveratrol in human melanoma cells sensitive or resistant to temozolomide. Melanoma Res. 2004a;14(3):189–96.
27. Giaever I, Keese C. Monitoring fibroblast behavior in tissue culture with an applied electric field. Proc Natl Acad Sci. 1984;81(12): 3761–4.
28. Gokce, E., Korkmaz, E., Dellera, E., Sandri, G., Bonferoni, C. and Ozer, O. (2019). Resveratrol-loaded solid lipid nanoparticles versus nanostructured lipid carriers: evaluation of antioxidant potential for dermal applications, 7, 1841–1850.
29. Gui F, Ma W, Cai S, Li X, Tan Y, Zhou C, et al. Preliminary study on molecular mechanism of curcumine anti-mouse melanoma. Pubmed. 2008;31(11):1685–9.
30. Gupta, S., Kesarla, R., Chotai, N., Misra, A., & Omri, A. (2017). Systematic approach for the formulation and optimization of solid lipid nanoparticles of efavirenz by high pressure homogenization using design of experiments for brain targeting and enhanced bioavailability. BioMed Research international, 2017.
31. Heenatigala Palliyage G, Singh S, Ashby C, Tiwari A, Chauhan H. Pharmaceutical topical delivery of poorly soluble polyphenols: potential role in prevention and treatment of melanoma. AAPS PharmSciTech. 2019;20(6):1–24.
32. Heijink IH, Brandenburg SM, Noordhoek JA, Postma DS, Slebos D, van Oosterhout AJM. Characterisation of cell adhesion in airway epithelial cell types using electric cell-substrate impedance sensing. Eur Respir J. 2010;35(4):894–903.
33. Heurtault B, Saulnier P, Pech B, Proust JE, Benoit JP. Physico-chemical stability of colloidal lipid particles. Biomaterials. 2003;24:4283–300.
34. Hu C, Wang Q, Ma C, Xia Q. Non-aqueous self-double-emulsifying drug delivery system: a new approach to enhance resveratrol solubility for effective transdermal delivery. Colloids Surf A Physicochem Eng Asp. 2016;489:360–9.
35. Hu L, Xing Q, Meng J, Shang C. Preparation and enhanced oral bioavailability of cryptotanshinone-loaded solid lipid nanoparticles. AAPS PharmSciTech. 2010;11(2):582–7.
36. Itoh T, Xia J, Magavi R, Nishihata T, Rytting JH. Use of shed snake skin as a model membrane for in vitro percutaneous penetration studies: comparison with human skin. Pharm Res. 1990;7: 1042–7.
37. Jayaprakasha GK, Chidambara Murthy KN, Patil BS. Enhanced colon cancer chemoprevention of curcumin by nanoencapsulation with whey protein. Eur J Pharmacol. 2016;789:291–300.
38. Jiang H, Shang X, Wu H, Gautam SC, Al-Holou S, Li C, et al. Resveratrol downregulates PI3K/Akt/mTOR signaling pathways in human U251 glioma cells. Journal of Experimental Therapeutics & Oncology. 2009;8(1):25–33.
39. Jiang, W. G. (2012). Electric cell-substrate impedance sensing and cancer metastasis (1st ed. 2012. Ed.) Dordrecht: springer Netherlands: imprint: springer.
40. Johnston ST, Shah ET, Chopin LK, Sean McElwain DL, Simpson MJ. Estimating cell diffusivity and cell proliferation rate by interpreting IncuCyte ZOOMTM assay data using the fisher-kolmogorov model. BMC Syst Biol. 2015;9(1):38.
41. Kleijn, A., Kloezeman, J. J., Balvers, R. K., Kaaij, M., Dirven, C. M. F., Leenstra, S., et al. (2016). A systematic comparison identifies an ATP-based viability assay as most suitable read-out for drug screening in glioma stem-like cells. *Stem Cells International*, *2016*.
42. Klein MC, Gorb SN. (2012) Epidermis architecture and material properties of the skin of four snake species. J R Soc Interface. 2012 Nov 7;9(76):3140–55. doi: 10.1098/rsif.2012.0479. Epub 2012 Aug 15. PMID: 22896567; PMCID: PMC3479930.
43. Kumpugdee-Vollrath, M., Subongkot, T., & Ngawhirunpat, T. (2013). Model membrane from shed Snake skins, International Journal of Pharmacological and Pharmaceutical Science, 7(10).
44. Lee J, Jang J, Park C, Kim B, Choi Y, Choi B. Curcumin suppresses α-melanocyte stimulating hormone-stimulated melanogenesis in B16F10 cells. Int J Mol Med. 2010;26(1):101–6.
45. Lei M, Dong Y, Sun C, Zhang X. Resveratrol inhibits proliferation, promotes differentiation and melanogenesis in HT-144 melanoma cells through inhibition of MEK/ERK kinase pathway. Microb Pathog. 2017;111:410–3. https://doi.org/10.1016/j.micpath.2017.09.029.
46. Lo C, Keese CR, Giaever I. Monitoring motion of confluent cells in tissue culture. Exp Cell Res. 1993;204(1):102–9. https://doi.org/10.1006/excr.1993.1014.
47. Loch-Neckel G, Santos-Bubniak L, Mazzarino L, Jacques AV, Moccelin B, Santos-Silva M, et al. Orally administered chitosan-coated polycaprolactone nanoparticles containing curcumin attenuate metastatic melanoma in the lungs. J Pharm Sci. 2015;104(10): 3524–34.
48. Lundien M, Mohammed K, Nasreen N, Tepper R, Hardwick J, Sanders K, et al. Induction of MCP-1 expression in airway epithelial cells: role of CCR2 receptor in airway epithelial injury. J Clin Immunol. 2002;22(3):144–52.
49. Majumdar APN, Banerjee S, Nautiyal J, Patel BB, Patel V, Du J, et al. Curcumin synergizes with resveratrol to inhibit colon cancer. Nutr Cancer. 2009;61(4):544–53.
50. Mazzarino L, Otsuka I, Halila S, Bubniak LDS, Mazzucco S, Santos-Silva MC, et al. Xyloglucan- block -poly(ϵ-Caprolactone) copolymer nanoparticles coated with chitosan as biocompatible mucoadhesive drug delivery system. Macromol Biosci. 2014;14(5): 709–19.
51. Naik B, Gandhi J, Shah P, Naik H, Sarolia J. Asenapine maleate loaded solid lipid nanoparticles for oral delivery. International Research Journal Of Pharmacy. 2017;8(11):45–53. https://doi.org/10.7897/2230-8407.0811216.
52. Naves LB, Dhand C, Venugopal JR, Rajamani L, Ramakrishna S, Almeida L. Nanotechnology for the treatment of melanoma skin cancer. Progress in Biomaterials. 2017;6(1):13–26.
53. Oliveira CP, Venturini CG, Donida B, Poletto FS, Guterres IS, Pohlmann AR. An algorithm to determine the mechanism of drug distribution in lipid-corenanocapsule formulations. Soft Matter. 2013;9:1141–50.
54. Opp, Daniel, "ECIS assessment of cytotoxicity and trans-endothelial migration of metastatic cancer cells" (2009). Graduate

Theses and Dissertations. http://scholarcommons.usf.edu/etd/2125
55. Pando D, Caddeo C, Manconi M, Fadda AM, Pazos C. Nanodesign of olein vesicles for the topical delivery of the antioxidant resveratrol. J Pharm Pharmacol. 2013;65(8):1158–67.
56. Pardeshi C, Rajput P, Belgamwar V, Tekade A, Patil G, Chaudhary K, et al. Solid lipid based nanocarriers: An overview / nanonosaci na bazi cvrstih lipida: Pregled. Acta Pharma. 2012;62(4):433–72.
57. Patel, Meghavi (2012) "Development, characterization and evaluation of solid lipid nanoparticles as a potential anticancer drug delivery system" Theses and Dissertations 400.
58. Pongjanyakul T, Prakongpan S, Priprem A. Permeation studies comparing cobra skin with human skin using nicotine transdermal patches. Drug Dev Ind Pharm. 2000;26(6):635–42.
59. Pushpalatha R, Selvamuthukumar S, Kilimozhi D. Comparative Insilico docking analysis of Curcumin and resveratrol on breast Cancer proteins and their synergistic effect on MCF-7 cell line. Journal of Young Pharmacists. 2017;9(4):480–5.
60. Pushpalatha R, Selvamuthukumar S, Kilimozhi D. Cyclodextrin nanosponge based hydrogel for the transdermal co-delivery of curcumin and resveratrol: development, optimization, *in vitro* and ex vivo evaluation. Journal of Drug Delivery Science and Technology. 2019;52:55–64.
61. Ray P, Yu H, Fu P. Toxicity and environmental risks of Nanomaterials: challenges and future needs. Journal of Environmental Science and Health, Part C. 2009;27(1):1–35.
62. Sahebkar A. Dual effect of curcumin in preventing atherosclerosis: the potential role of pro-oxidant–antioxidant mechanisms. Nat Prod Res. 2014;29(6):491–2.
63. Sambale F, Wagner S, Stahl F, Khaydarov R, Scheper T, Bahnemann D. Investigations of the toxic effect of silver nanoparticles on mammalian cell lines. J Nanomater. 2015;2015:1–9. https://doi.org/10.1155/2015/136765.
64. Saralkar P, Dash A. Alginate nanoparticles containing Curcumin and resveratrol: preparation, characterization, and in vitro evaluation against DU145 prostate Cancer cell line. AAPS PharmSciTech. 2017;18(7):2814–23. https://doi.org/10.1208/s12249-017-0772-7.
65. Schaefer H, Zesch A, Stuttgen G. Penetration, permeation, and absorption of triamcinolone acetonide in Normal and psoriatic skin. Archives for Dermatological Research. 1977;258(3):241–9.
66. Sengupta S, Banerjee S, Sinha B, Mukherjee B. Improved Skin Penetration Using In Situ Nanoparticulate Diclofenac Diethylamine in Hydrogel Systems: In Vitro and In Vivo Studies. AAPS PharmSciTech. 2016;17:307–17. https://doi.org/10.1208/s12249-015-0347-4.
67. Shah, R. (2016). Microwave-assisted production of solid lipid nanoparticles. (Doctodoctoral dissertations, Swinburne University of Technology).
68. Shelat P, Mandowara V, Gupta D, Patel S. Formulation of curcuminoid loaded solid lipid nanoparticles in order to improve oral bioavailability. Int J Pharm Pharm Sci. 2018;7(6).
69. Shenfield GM. Fixed combination drug therapy. Drugs. 1982;23(6):462–80.
70. Siepmann, J., & Siepmann, F. (2011). Mathematical modeling of drug release from lipid dosage forms doi:https://doi.org/10.1016/j.ijpharm.2011.07.015.
71. Single A, Beetham H, Telford BJ, Guilford P, Chen A. A comparison of real-time and endpoint cell viability assays for improved synthetic lethal drug validation. J Biomol Screen. 2015;20(10):1286–93.
72. Siwak DR, Shishodia S, Aggarwal BB, Kurzrock R. Curcumin-induced antiproliferative and proapoptotic effects in melanoma cells are associated with suppression of IκB kinase and nuclear factor κB activity and are independent of the B-Raf/mitogen-activated/extracellular signal-regulated protein kinase pathway and the akt pathway. Cancer. 2005;104(4):879–90.
73. Souto EB, Mehnert W, Müller RH. Polymorphic behaviour of Compritol®888 ATO as bulk lipid and as SLN and NLC. J Microencapsul. 2006;23(4):417–33.
74. Sugimoto T. Chapter 4 - recrystallization. Monodispersed Particles. 2001:139–54. https://doi.org/10.1016/B978-044489569-1/50022-1.
75. Sun C, Wu MH, Guo M, Day ML, Lee ES, Yuan SY. ADAM15 regulates endothelial permeability and neutrophil migration via Src/ERK1/2 signalling. Cardiovasc Res. 2010;87(2):348–55.
76. Sun, Y., Du, L., Liu, Y., Li, X., Li, M., Jin, Y., et al.(2014). Transdermal delivery of the in-situ hydrogels of curcumin and its inclusion complexes of hydroxypropyl-β-cyclodextrin for melanoma treatment doi:https://doi-org.cuhsl.creighton.edu/10.1016/j.ijpharm.2014.04.039.
77. Szulcek, R., Bogaard, H. J., & van Nieuw Amerongen, G.,P. (2014a). Electric cell-substrate impedance sensing for the quantification of endothelial proliferation, barrier function, and motility. Journal of Visualized Experiments: JoVE, (85).
78. Szulcek, R., Bogaard, H. J., & van Nieuw Amerongen, G.,P. (2014b). Electric cell-substrate impedance sensing for the quantification of endothelial proliferation, barrier function, and motility. Journal of Visualized Experiments: JoVE, (85).
79. Tang J, Ji H, Ren J, Li M, Zheng N, Wu L. Solid lipid nanoparticles with TPGS and Brij 78: a co-delivery vehicle of curcumin and piperine for reversing P-glycoprotein-mediated multidrug resistance in vitro. Oncol Lett. 2017;13(1):389–95. https://doi.org/10.3892/ol.2016.5421.
80. Uner M. Preparation, characterization and physico-chemical properties of solid lipid nanoparticles (SLN) and nanostructured lipid carriers (NLC): their benefits as colloidal drug carrier systems. Pharmazie. 2006;61(5):375–86.
81. Wang B, Liu X, Teng Y, Yu T, Chen J, Hu Y, et al. Improving anti-melanoma effect of curcumin by biodegradable nanoparticles. Oncotarget. 2017a;8(65):108624–42.
82. Wang B, Liu X, Teng Y, Yu T, Chen J, Hu Y, et al. Improving anti-melanoma effect of curcumin by biodegradable nanoparticles. Oncotarget. 2017b;8(65):108624–42.
83. Wang M, Yu T, Zhu C, Sun H, Qiu Y, Zhu X, et al. Resveratrol triggers protective autophagy through the Ceramide/Akt/mTOR pathway in melanoma B16 cells. Nutrition & Cancer. 2014;66(3):435–40.
84. Wichitnithad W, Nimmannit U, Callery PS, Rojsitthisak P. Effects of different carboxylic ester spacers on chemical stability, release characteristics, and anticancer activity of mono-PEGylated curcumin conjugates. J Pharm Sci. 2011;100(12):5206–18.
85. Wu Z, Liu BEC, Liu J, Zhang Q, Liu J, Chen N, et al. Resveratrol inhibits the proliferation of human melanoma cells by inducing G1/S cell cycle arrest and apoptosis. Mol Med Rep. 2014;11(1):400–4.
86. Ying X, Cui D, Yu L, Du Y. Solid lipid nanoparticles modified with chitosan oligosaccharides for the controlled release of doxorubicin. Carbohydr Polym. 2011;84(4):1357–64.
87. Zang Y, Hao D, Wang H, Yang Z, Liu H, Zhang S. Structure-based methoxyflavone derivatives with potent inhibitory activity against various influenza neuraminidases. J Biomol Struct Dyn. 2019;15:1–10. https://doi.org/10.1080/07391102.2019.1680436.